



Illinois Institute of Technology Chicago, Illinois

**INTERACTIONS BETWEEN FRICTION-INDUCED
VIBRATION AND WEAR**

**FINAL REPORT
FOR PERIOD MAY 15, 1982 - MAY 15, 1984**

**A.F. D'SOUZA, V. ARONOV, S. KALPAKJIAN,
I. SHAREEF AND A.H. DWEIB**

JANUARY 1985

**PREPARED FOR
THE U. S. DEPARTMENT OF ENERGY
AGREEMENT No. DE-AC02-82ER12071**

INTERACTION BETWEEN FRICTION-INDUCED
VIBRATION AND WEAR

Final Report

For Period May 15, 1982 - May 15, 1984

A.F. D'Souza, V. Aronov, S. Kalpakjian,
I. Shareef and A.H. Dweib

Illinois Institute of Technology
Chicago, Illinois 60616

JANUARY 1985

Prepared for
The U. S. Department of Energy
Agreement No. DE-AC02-82ER12071

N O T I C E

This report was prepared as an account of work sponsored by the United States Government. Neither the United States nor the Department of Energy, nor any of their employees, nor any of their contractors, subcontractors, or their employees, make any warranty, express or implied, or assumes any legal liability or responsibility for the accuracy, completeness, or usefulness of any information, apparatus, product or process disclosed or represents that its use would not infringe privately-owned rights.

TABLE OF CONTENTS

Abstract	Page
I. Introduction	1
II. Experimental Set-up and Results	4
III. Modification of Experimental Set-up	14
IV. Analysis of Self-Excited Vibrations	21
V. Summary and Conclusions	40
Acknowledgments	43
References	44
Appendix 1	
Appendix 2	
Appendix 3	
Appendix 4	

Abstract

The interactions among friction, wear, and system dynamics have been investigated for dry sliding contact between a steel pin and a cast iron disk. The system was equipped with force and displacement transducers to measure the contact forces and the displacements in three directions.

As the normal load increased, four different regimes were observed, the steady state friction regime, the nonlinear friction regime, transient friction regime, and the self-excited vibration regime.

The last regime is characterized by periodic oscillations of the slider and high wear rate. The experimental setup was modified for further detailed study of this regime.

The recorded wave forms showed that the oscillations consist of a fundamental harmonic with a frequency close to the system natural frequency in torsion and its second harmonic. A mathematical model was developed for the system including the coupling between the different degrees of freedom and a nonlinear contact stiffness, and the model was analyzed using triple input describing functions to include the constant, fundamental, and second harmonics.

The model showed the existence of limit cycling at a

frequency close to the torsional frequency of the system with amplitudes close to those observed experimentally. The results of this study enhance our understanding of friction induced vibrations and interactions which give rise to instability.

I. INTRODUCTION

The subject of tribology is being increasingly recognized as an important area of study due to its great economic impact. Friction and wear between sliding surfaces has been studied for many years by several investigators in the past in terms of their controlling factors and parameters such as materials, surface conditions, loads, speed, temperature and lubricants. Various theories have been proposed concerning the mechanisms of friction and wear and this has led to the establishment of a significant body of knowledge concerning tribology.

However, the effect of the dynamic characteristics of the equipment or machine on sliding frictional contact and wear is a sub-area of tribology which is still poorly understood. One aspect of the interaction between friction and stiffness that has received separate attention in the past is vibrations induced by friction. Different types of vibrations induced by friction have been studied by several investigators including Soom & Kim [1], Ko & Brockley [2], Krauter [3], Earles & Lee [4] and the present authors [5,6,7,8].

However, there is still a lack of knowledge at the present time concerning various interactions among friction, wear and system stiffness. It is recognized that the system stiffness has a significant effect on friction and wear. In his studies of sliding friction and wear of lubricated steel surfaces, Zaporozetz [9,10] has observed that the transition from mild to severe wear is accompanied by a change in the amplitude

and frequency of the friction force oscillations. Rice, et al. [11] have investigated sliding and impact wear and have observed that different wear behaviors can result from variation in the specimen length which, in their setup, corresponds to variation in stiffness.

Kato, et al. [12] have investigated the effect of system stiffness on wear and vibrations. They concluded that wear of steel against steel is higher for a stiff system as compared to that obtained for an elastic system; whereas, for frictional pairs, such as bronze-steel and white metal-steel, wear tends to decrease with increasing stiffness. Investigating the effect of contact vibrations, Miyagawa, et al. [13] showed that frictional vibrations increased wear. The subject of normal vibrations and stiffness on contact friction has been investigated by several authors [14-17] and occasionally a reference to vibrational or stiffness phenomenon in simulative wear testing is also found in the literature [18]. However, no attempt has been made to investigate wear mechanisms and relate them to the kinetics of fracture processes on the frictional surfaces in order to find causes of the system stiffness effect on wear.

It is apparent that there are complex interrelationships among friction, wear and vibrations and different friction and wear mechanisms may be operative under certain conditions. But the interactions are not clearly understood and the condition under which transition takes place from one type of behavior to another are difficult to establish.

Under sponsorship of the Office of Energy Research of the U.S. Department of Energy, the present authors have been conducting a systematic investigation of the effect of system rigidity on friction and wear in the Tribology Laboratory of IIT. Dry frictional contact between two metallic surfaces, one cast iron and the other steel, was investigated. The objectives of the study were the following: 1). Investigation of the different regions of friction, wear, and vibrations as influenced by the normal load and system stiffness; 2). Modeling of wear in the mild wear region as influenced by contact vibrations and system stiffness; 3). Analysis of the region of self-excited vibrations.

II. EXPERIMENTAL SET-UP AND RESULTS

Apparatus. Measurements were made with a pin-on-disc type sliding friction apparatus instrumented with piezoelectric force and acceleration transducers. A general view of the test apparatus is shown in Fig. 1, and an extensive description of the associated instrumentation is given in Appendix 1. Briefly stated, the apparatus consists of a rotating disc, 200 mm in diameter, driven by a 1 HP AC motor through a variable-speed drive which gives a speed range from 0 to 700 RPM.

The pin, which represents a stationary mating surface is 5 mm in diameter. An expansion bolt serves to grip the pin at one end and an accelerometer at the other, while the force transducer is sandwiched with preload of 25 KN between bolt head and supporting arm. The supporting arm, whose length can be varied by changing the position of the clamp, is used as a spring with variable stiffness. Strain gages fixed on the supporting arm were used to record continuously the friction force f_x , on a strip chart recorder. The variations in the friction force F_x and normal force F_z were sensed by piezoelectric transducers and were recorded on a visicorder.

Materials. A special quality steel 0.5% C, 0.85% Mn, 0.04% P and 0.05% S, quenched and hardened to 48 HRC was used as pin material. The material of the disc was cast iron.

Test Procedure. The pin and disc were lapped in situ with 600 grit lapping compound to a smooth finish (0.5 μ m CLA) under a normal load of 8 N (1.8 lb). Special care

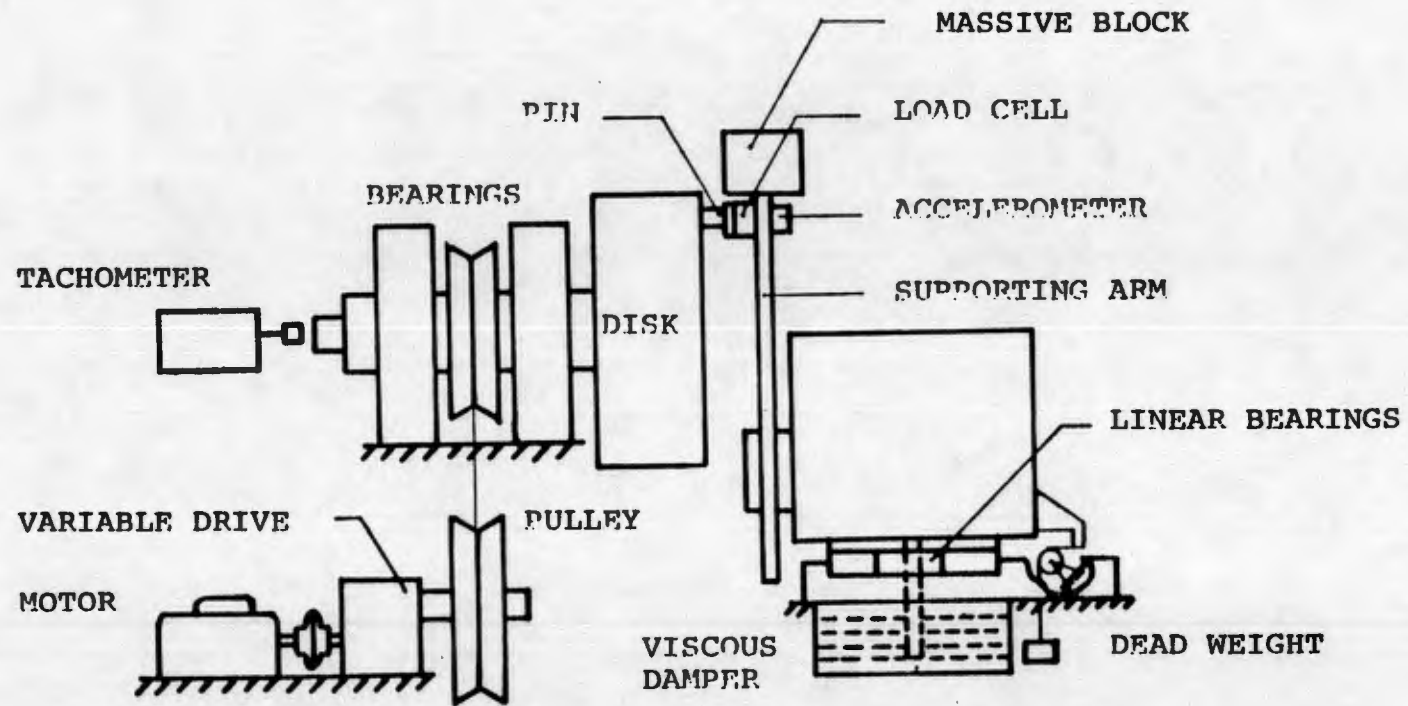


Fig. 1

was taken to ensure clean surfaces by cleaning with methanol and acetone. The pin was brought in contact with the revolving disc at 8 N normal load and, in this state, the pin was allowed to run in for a distance of approximately 12-15 Km to ensure that a stable steady state friction process had been achieved. After this, the normal load was increased in steps of 4.5 N (1 lb) up to a load of 26 N and then the load was increased in steps of 9 N (2 lbs). The time between any two consecutive loadings was maintained at around thirty minutes.

At each normal load, the analog wave form of the dynamic components, F_x and F_z in frictional and normal forces and the corresponding velocities V_x and V_z were recorded on a visicorder oscillograph. A spectral analyzer was used to analyze the analog signals to obtain the spectra SF_x , SF_z , SV_x and SV_z of forces F_x , F_z and velocities V_x , V_z , respectively.

Three sets of experiments were conducted for supporting arm lengths of 5.1 cm (2 in), 8.9 cm (3.5 in), 12.7 cm (5 in) corresponding to stiffnesses K_1 , K_2 and K_3 , respectively, in decreasing order. All sets of experiments have been repeated at least two times. In all experiments reported here, the sliding speed was maintained constant at 46 cm/s. For each arm length, the rate and magnitude of normal loading and the recording of various parameters at each load were performed in the same manner as stated in the preceeding. All experiments were performed in ambient environment where the temperature ranged from 20 to 23° C (68 to 73° F) and

relative humidity from 50 to 60%.

Experimental Results

Four different regimes of behavior were observed depending on the normal load and stiffness. These regimes are shown in Fig. 2 for stiffness K_1 (most stiff) and in Fig. 3 for stiffness K_3 (least stiff). They are classified as steady state friction region, nonlinear friction region, transient friction region with disturbances, and self-excited vibration region. The detailed behavior in these four regions is described in the following, and further details are given in Appendix 2.

Steady State Friction Region. In this region, which is encountered for low values of the normal load, the friction force increases linearly with the normal load. The mean value of the friction force remains constant between loadings. Small oscillations in the forces and slider velocities are observed. Their amplitudes decrease with increasing normal load. The variation of wear, roughness, and amplitude of normal force oscillations are given in Figs. 4, 5, and 6. Analysis of these data has shown that the increase in wear with stiffness is only associated with a change in the frequency of oscillation of the supporting arm. The shorter the arm the higher the frequency of oscillation. This effect of frequency on the wear rate was explained by relating wear to the number of loading cycles. The increase in frequency of normal load oscillation causes an increase in number of loading

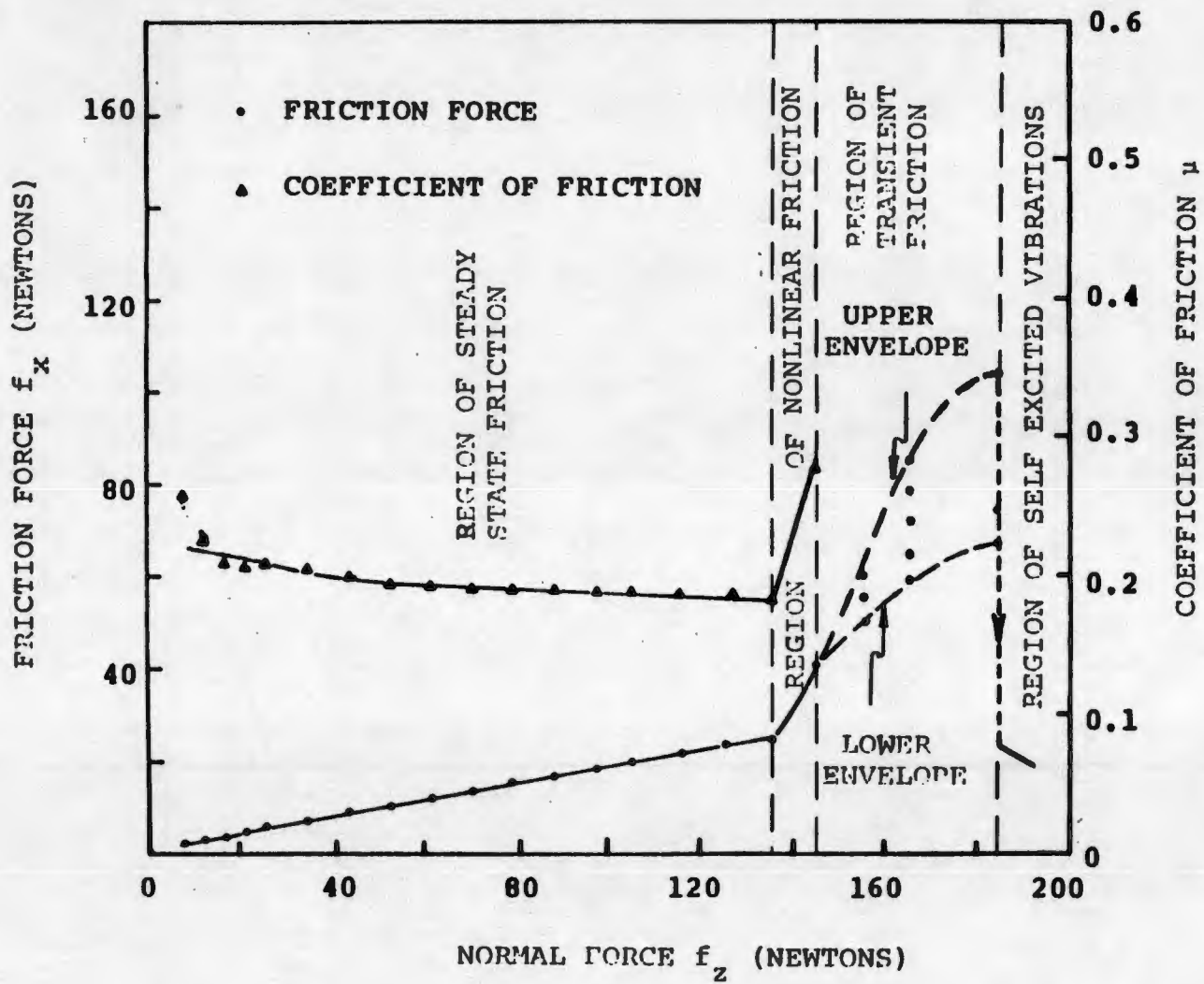


Fig. 2. Friction force vs. normal force showing various regions of friction

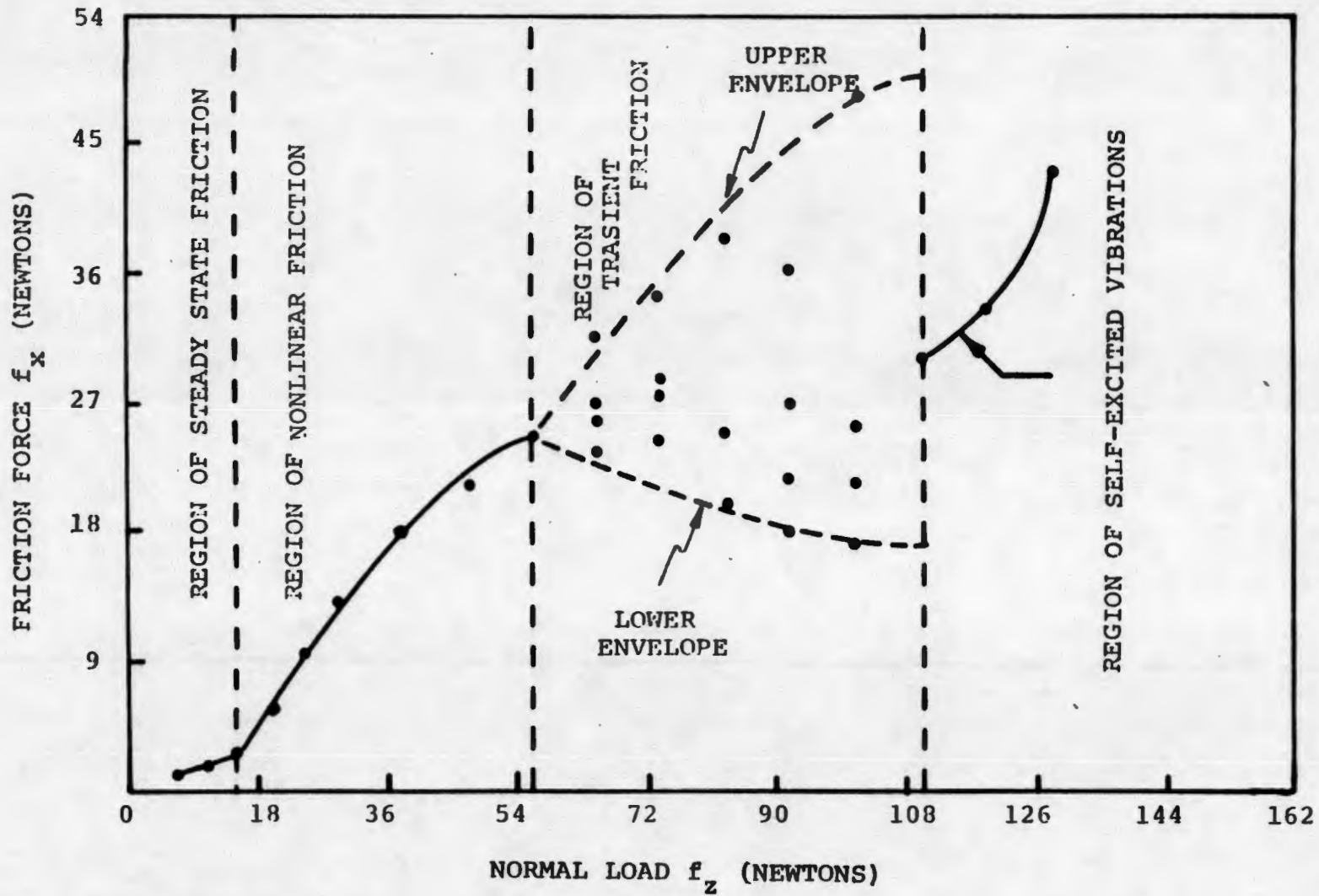


Fig.3 Friction force vs. normal force showing various regions of friction

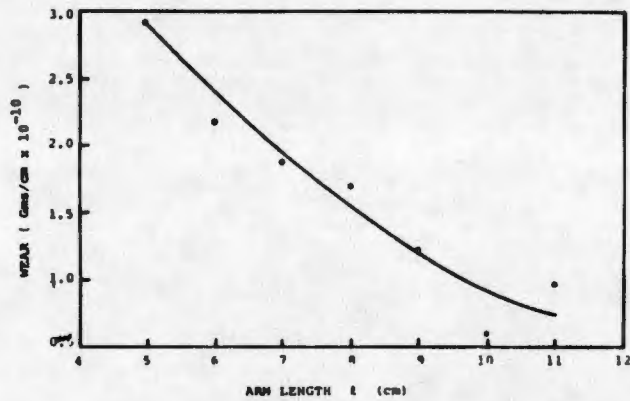


Fig. 4 Wear per unit sliding distance vs. supporting arm length

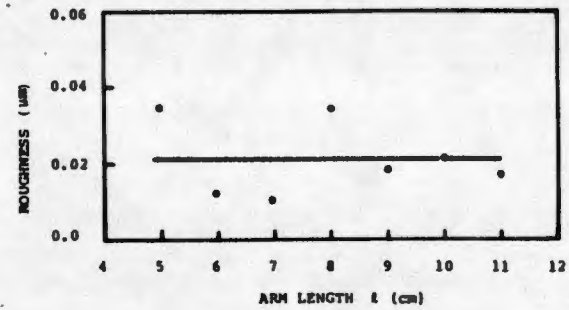


Fig. 5 Surface roughness along the direction of travel vs. supporting arm length

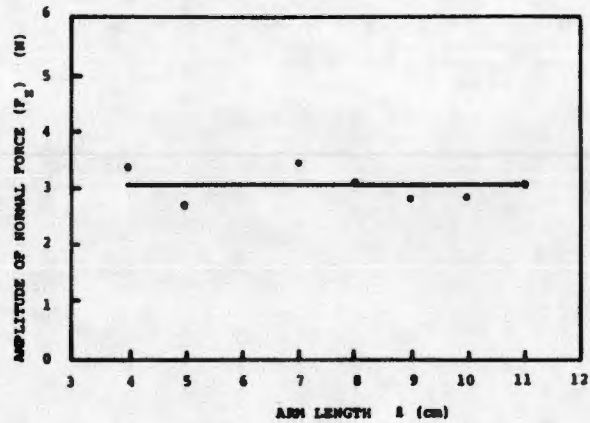


Fig. 6 Amplitude of normal force oscillation vs. supporting arm length

cycles per unit time. In this case, the most probable mechanism of wear particles formation is a fatigue mechanism. On the basis of these findings an analytical wear model was developed that accounted for slider oscillation in the normal direction [8] and the details are given in Appendix 4. At a critical value of the normal load, which depends on the system stiffness, transition occurs from the steady state friction region to the nonlinear friction region. The transition from steady state friction also corresponds to the transition from mild to severe wear. This transition in wear is an important tribological consideration because dry sliding contact bearings, guides, cams and other frictional elements are required to operate in the region of mild wear.

The effect of the system stiffness on the critical normal load at which transition takes place in friction, wear and vibrations is seen by comparing Figs. 2 and 3. For the stiffest system of Fig. 2, the critical normal load for transition is about 136 N whereas for the least stiff system of Fig. 3, the critical normal load has been reduced drastically to only about 15 N. The critical load is seen to be proportional to the square of the system natural frequency.

Nonlinear Friction Region. In this region, the friction force increases nonlinearly with the normal load. The coefficient of friction is no longer constant and independent of the normal load but increases with it. The mean value of the friction force remains constant between loadings as in the first region. But the mean values of the amplitudes of the oscillations in

the forces and velocities increase with increasing normal load.

A light microscope analysis and surface profilometry indicates that after the transition, the surface becomes gradually damaged and the roughness increases with the normal load.

Region of Transient Friction with Disturbances. When the normal load lies in the range from 146 to 185 N for the stiffest system of Fig. 2 and from 56 to 110 N for the least stiff system of Fig 3, we observe a region of transient friction. In this region, the mean value of the friction force does not remain constant with time for a constant value of the normal load. It increases with time until it reaches a sufficiently high value when a burst of self-excited vibrations occur. The friction force instantly falls to a lower value, the self-excited vibrations disappear and the process is repeated. The upper and lower envelopes of the mean value of the friction force are shown in Figs. 2 and 3. The mean value of the friction force lies within this envelope at a given time and hence in this region, it is not possible to define a mean value of the coefficient of friction.

Region of Self-Excited Vibrations. A region of self-excited vibrations is observed when the normal load is increased beyond 185 N in Fig, 2 and beyond 110 N in Fig. 3. The oscillations in the forces and slider displacement components are periodic and have the same fundamental frequency which corresponds to the torsional frequency of the system about the longitudinal axis of the slider arm. It is observed that

the wave-forms of the slider velocities are nearly sinusoidal but the wave-forms of the normal and friction forces have significant second harmonic components.

These self-excited vibrations have been analyzed by the principal investigators in reference [7] and the details are given in Appendix 3. It is shown that the coupling among the different degrees of freedom is an important consideration in self-excited vibrations. The energy supplied to maintain the vibrations is through the torsional mode which is mainly responsible for the cause of the self-excited vibrations. For further study of self-excited vibrations, some modifications were made to the experimental set-up of Chapter I. These modifications are described in the following chapter and further study of self-excited vibrations is given in Chapter IV.

III. MODIFICATION OF EXPERIMENTAL SET-UP

The test apparatus described in Chapter II was modified in order to conduct further detailed study of self-excited vibrations. The piezoelectric force transducer shown in the set-up of Fig. 1 measures only the dynamic components F_x and F_z of the contact forces in the frictional and normal directions, respectively. It is not capable of measuring the steady state force components. Also, it is necessary to avoid any effect of the inertial forces on the measurement of the contact forces.

For these reasons, the pin was mounted on a special dynamometer which was designed and fabricated to avoid cross sensitivity between the two components of the force. The dynamometer was fabricated from 4340 steel with no heat treatment. The principle of its operation is based on double cantilevers carrying tension and compression strain gages. The normal force F_z with its moment arm L_z shown in Fig. 7 causes a bending moment M_z on the vertical members only whereas the friction force F_x with its moment arm L_x causes a bending moment M_x on the horizontal members only.

The resistance gages G_1, G_2, G_3 and G_4 measure the bonding strain caused by the normal force. The gages G_1 and G_3 are in compression while gages G_2 and G_4 are in tension. Similarly, four strain gages G_5, G_6, G_7 and G_8 strain in Fig. 7 measure the bending strain caused by the friction force. The bridge connections are shown in Fig. 8. The gages are temperature compensated since tension and compression gages acting in a similar environment are connected to the bridge.

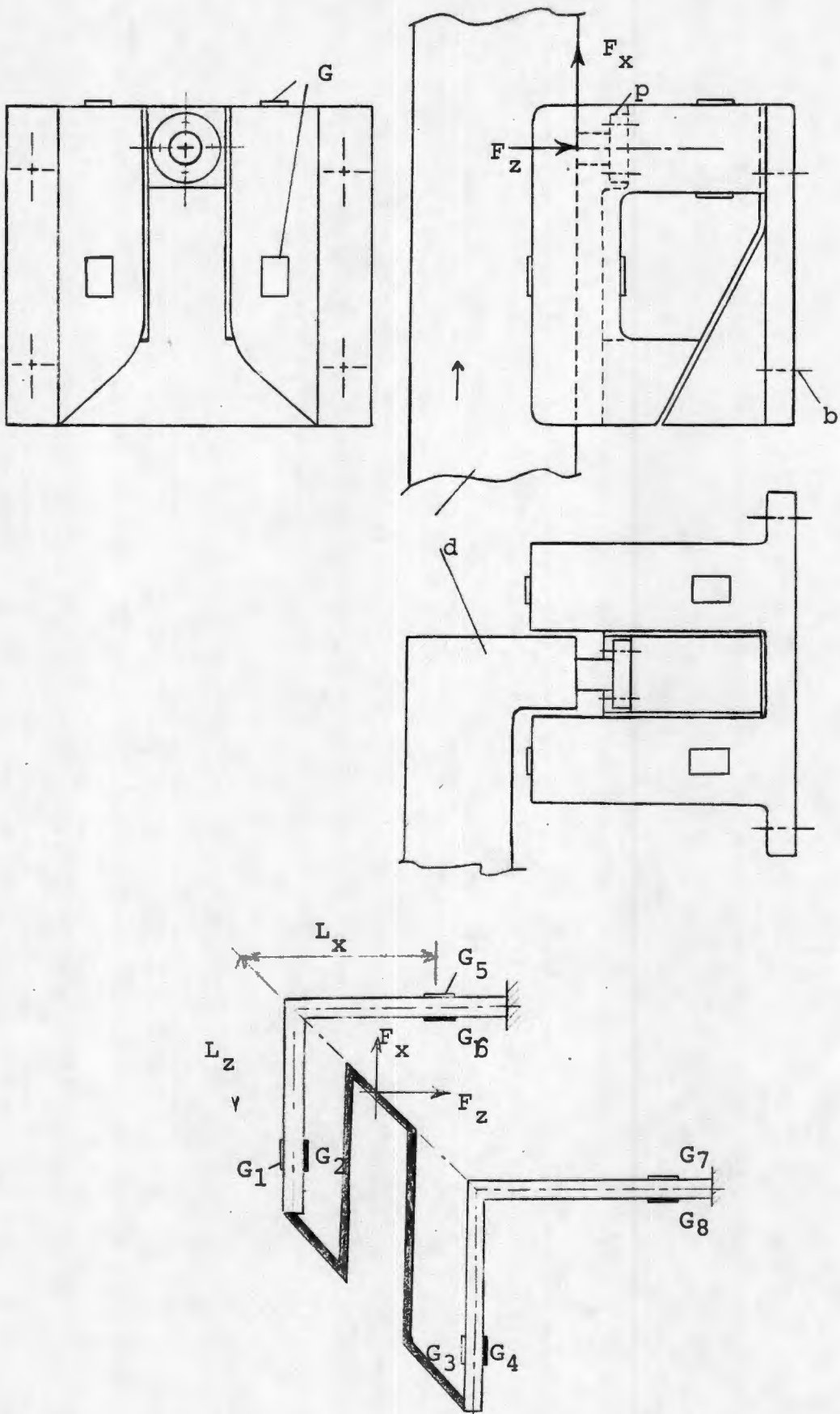


Fig. 7

The dynamometer was mounted on an arm which was clamped to a massive block as shown in Fig. 9. The arm serves as the spring and its stiffness can be altered by changing the distance between the clamp and the pin. The pin was fixed to the dynamometer with its axis parallel to the horizontal members of the double cantilever. The contact surface between the pin and the disk was made to lie along the axis of the vertical members as shown in Fig. 7.

The static tests conducted on the dynamometer indicated a cross sensitivity between 3 and 4 percent. The natural frequency of the dynamometer was found to be approximately 900 Hz which is well above the frequencies of vibrations.

The output of each bridge was amplified by an operational amplifier and then recorded on a Visicorder oscillograph. The dynamometer was calibrated by applying known dead weights in the appropriate directions in place of the contact forces and the output signal was recorded as a displacement on the Visicorder. The results show a linear relationship between the applied forces and the measured signals.

A triaxial accelerometer was mounted on the arm as shown in Fig. 9 at the level of the pin but on opposite side of the dynamometer. This accelerometer was employed to measure the vibrations in the normal and frictional directions. Since the torsional vibrations play an important role in self-excited vibrations, provision was made to measure the twist angle ϕ of the arm. The arm originally had a square cross section throughout its length. A part of the length of

the arm was given a round cross section and four strain gages were mounted on the surface of that part. The grid of each gage made an angle of 45° to the axis of the arm as shown in Fig. 10.

Thus the angle of twist of the arm was obtained by measuring the torque transmitted by the arm. The relationship between the twist angle ϕ and the torque T for the circular cross section is given by $T = k_T \phi$ where k_T is the torsional stiffness of the arm. The torsional strain gages were connected through a Wheatstone bridge and the bridge output was first amplified and then recorded on the Visicorder.

A special gig was constructed to calibrate the twist angle. A known dead weight with a moment arm produced a known torque T about the longitudinal axis of the arm. The angle of twist was magnified and measured with a micrometer. The results yielded a linear relationship between the applied torque T and the twist angle ϕ as shown in Fig. 11. The slope of this straight line is the torsional stiffness of the arm and has a value of $k_T = 1211.5 \text{ N}\cdot\text{m}/\text{rad}$. The bridge output was also recorded as a displacement on the Visicorder so that the amplitude of the waveform of the torsional vibrations could be obtained directly in radians from the Visicorder record.

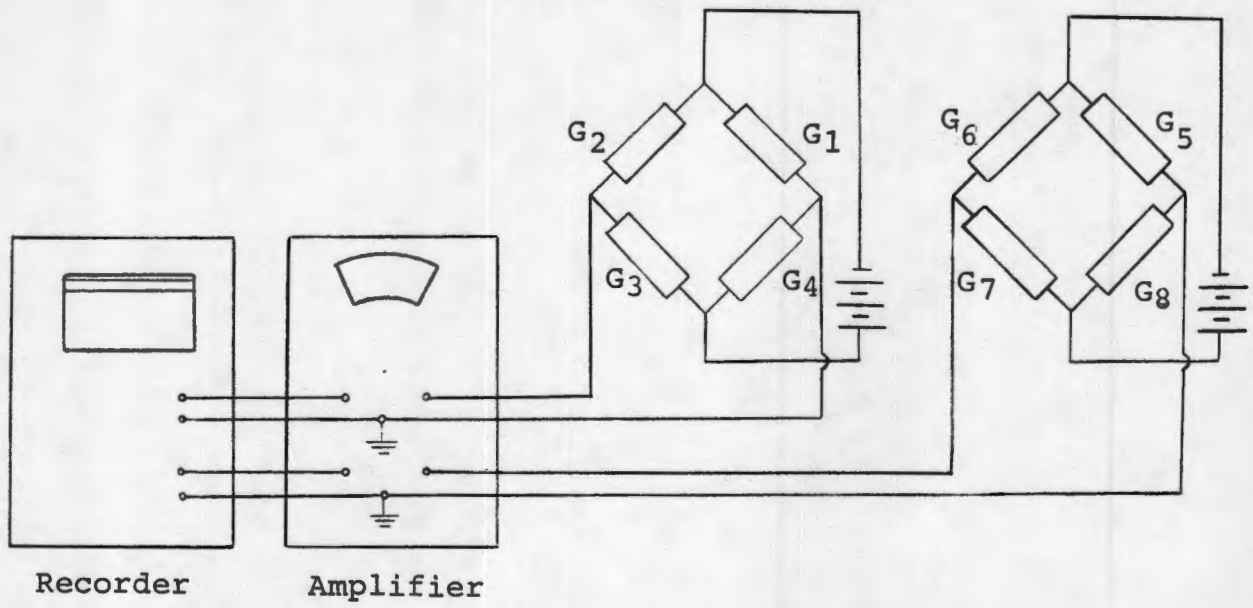
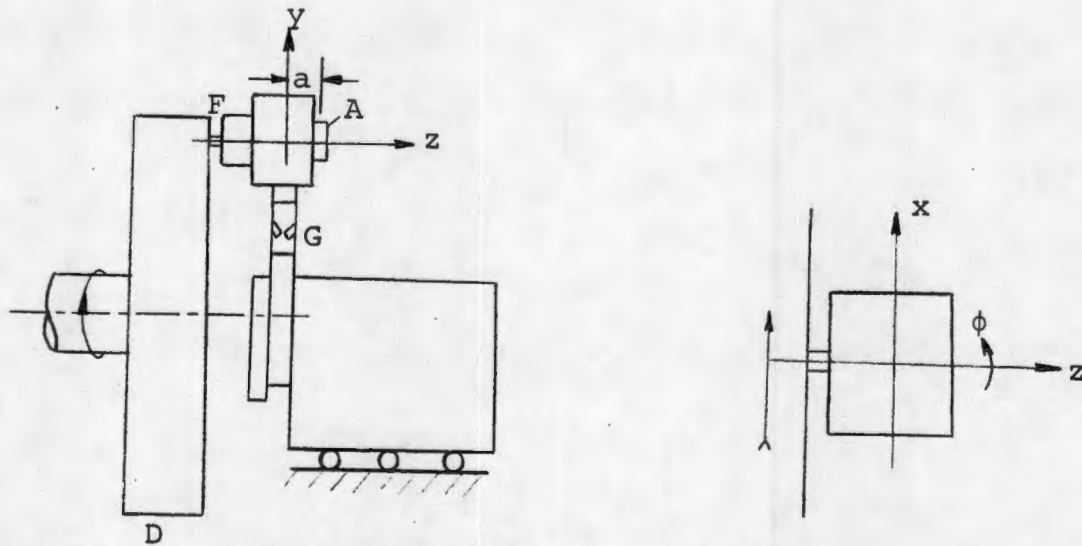
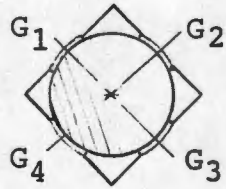


Fig. 8



F = Force transducer
A = Accelerometer
G = Torsional Strain Gages
D = Disc

Fig. 9



Section A-A

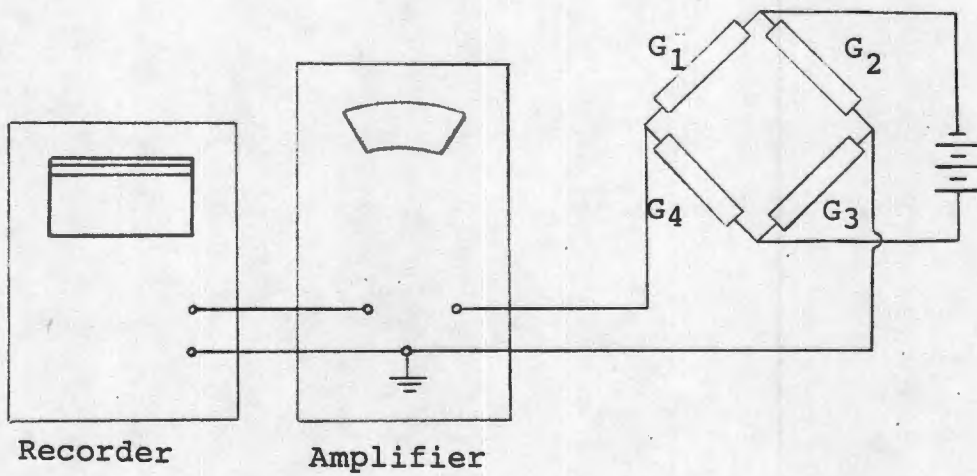
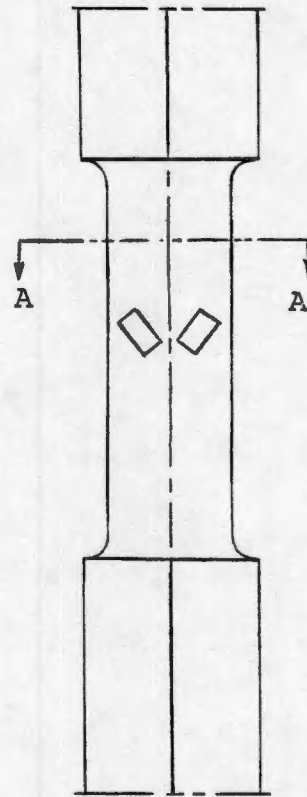


Fig. 10

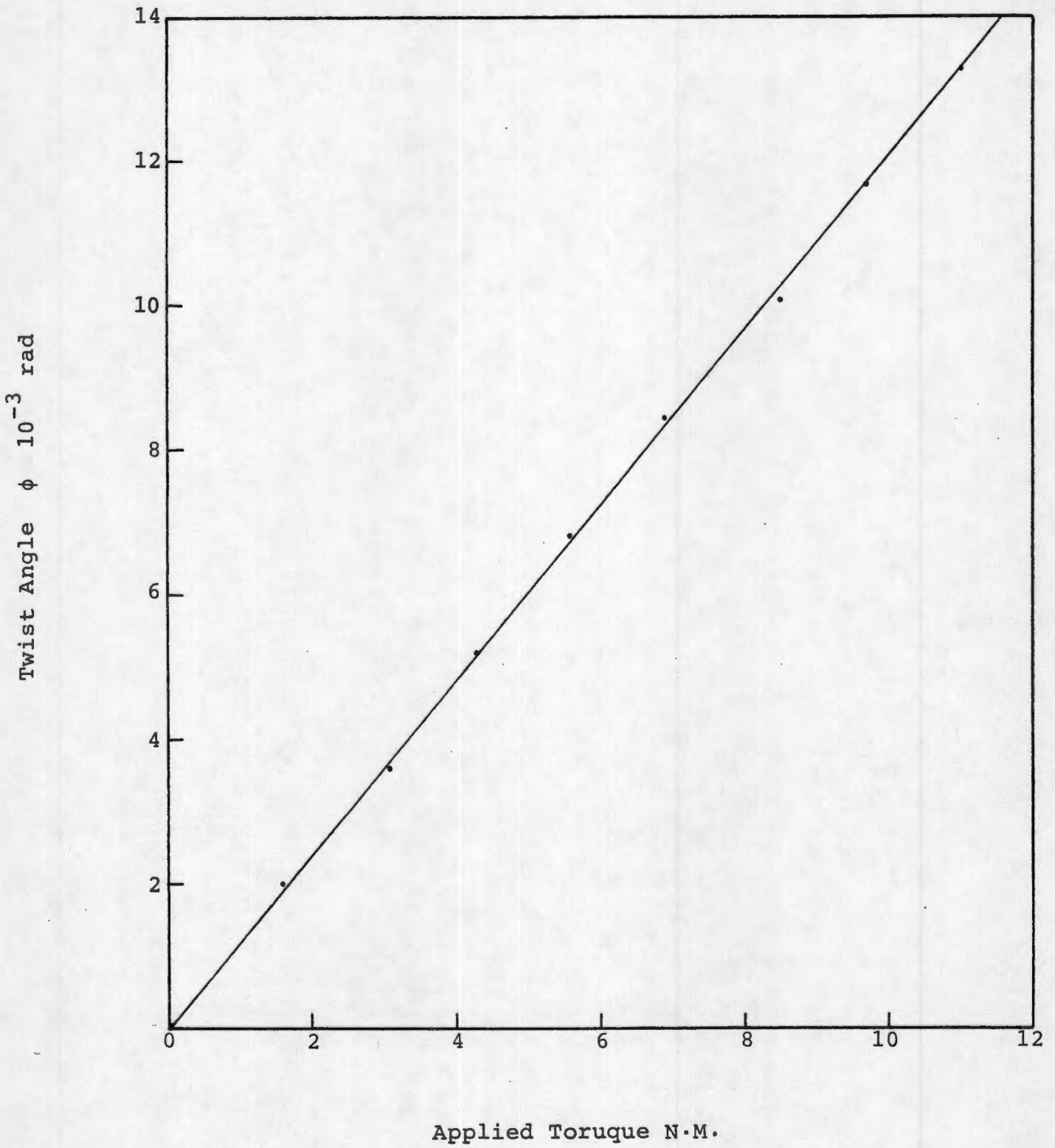


Figure 11 Torsional Stiffness of the Arm

IV. ANALYSIS OF SELF-EXCITED VIBRATIONS

Several experiments were conducted employing the experimental set-up described in the previous section. As the normal load was increased, the region of self-excited vibrations occurred at a certain critical value of the normal load. As stated previously for this region, the oscillations in the force and slider displacement components are periodic and have the same fundamental frequency which corresponds to the torsional frequency of the system about the longitudinal axis of the slider arm.

The waveforms of the force components F_z and F_x in the normal and frictional directions as measured by the dynamometer were recorded on the Visicorder. At the same time, the waveforms of the velocity components V_z and V_{xa} in the normal and friction directions as measured by the accelerometer and the twist angle ϕ obtained from the torsion strain gages were also recorded on the Visicorder.

Typical samples of the waveforms are shown in Fig. 12. In these experiments, the normal load was 84.5 N (19 lbs). The arm length was such that, when the slider is not in contact with the disk, the natural frequencies of free vibrations were $\omega_z = 55.00$ Hz, $\omega_x = 48.75$ Hz, and $\omega_t = 98.75$ Hz in the normal, frictional, and torsional directions, respectively. The corresponding damping ratios were $\zeta_z = 0.01129$, $\zeta_x = 0.00378$, and $\zeta_t = 0.00253$. The natural frequencies and damping ratios were obtained experimentally by employing a spectral analyzer.

It should be noted that Fig. 12 shows the waveform of

V_{xa} which is the velocity component in the frictional direction as measured by the accelerometer which was located at a distance $a = 18.5$ mm from the vertical axis of the arm as shown in Fig. 9. Hence, the waveform of the velocity component in the friction direction without the effect of torsional oscillations is obtained from

$$V_x = V_{xa} - a\dot{\phi} \quad (1)$$

It is seen that the waveforms of V_{xa} and ϕ are sinusoidal but those of F_z , F_x and V_z contain higher harmonics.

The waveforms were digitized and a computer program was written to obtain their Fourier series decomposition.

The Fourier series expansions yielded the following results.

$$F_z = 11.546 \sin(\omega t + 152.03^\circ) + 8.264 \sin(2\omega t - 128.83^\circ) \text{ N} \quad (2)$$

$$F_x = 2.486 \sin(\omega t + 146.48^\circ) + 2.930 \sin(2\omega t - 137.92^\circ) \text{ N} \quad (3)$$

$$V_z = 9.515 \sin(\omega t + 63.38^\circ) + 2.893 \sin(2\omega t + 139.61^\circ) \text{ mm/s} \quad (4)$$

$$V_{xa} = 15.898 \sin(\omega t - 119.51^\circ) \text{ mm/s} \quad (5)$$

$$\phi = 1.540 \sin(\omega t + 149.99^\circ) 10^{-3} \text{ rad/s} \quad (6)$$

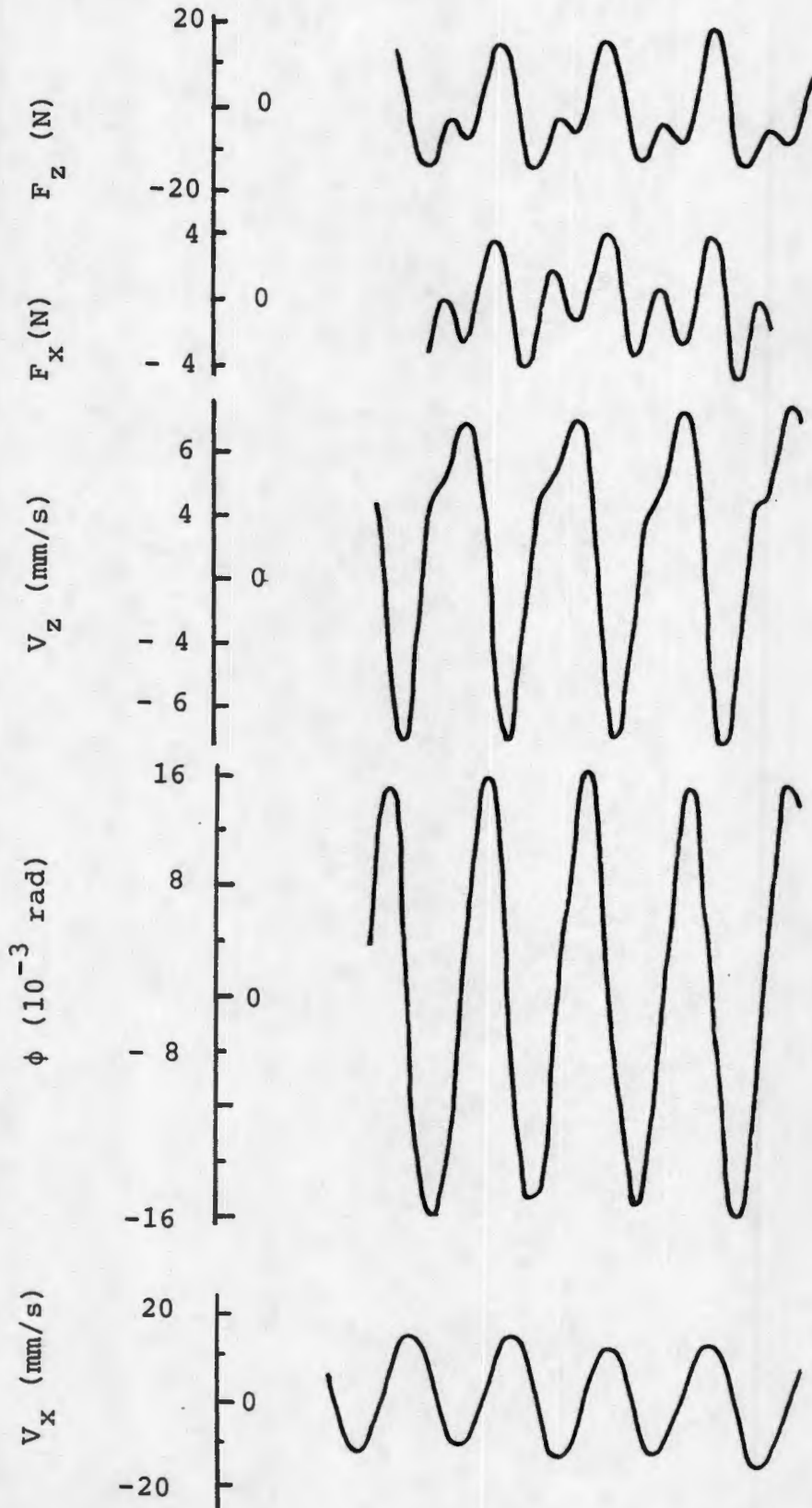
Where the fundamental frequency of oscillations was obtained as $\omega = 644.026$ rad/s (102.5 Hz). Substituting from (5) and (6) in (1), the velocity component in the frictional direction without the effect of torsional oscillations is given by

$$V_x = 2.455 \sin(\omega t + 56.75^\circ) \text{ mm/s} \quad (7)$$

Integrating (4) and (7) with respect to time, the corresponding displacements are

$$z = 14.774 \sin(\omega t - 26.62^\circ) + 2.248 \sin(2\omega t + 49.61^\circ) 10^{-6} \text{ m} \quad (8)$$

$$x = 3.813 \sin(\omega t - 33.25^\circ) 10^{-6} \text{ m} \quad (9)$$



Wave forms of self-excited vibration

Choosing the starting time such that the phase angle of the fundamental component of F_z is zero, that is, replacing ωt by $\omega t + 26.6^\circ$, we obtain the following results:

$$F_z = 11.546 \sin(\omega t + 178.65^\circ) + 8.264 \sin(2\omega t - 75.59^\circ) \text{ N} \quad (10)$$

$$F_x = 2.486 \sin(\omega t + 173.10^\circ) + 2.930 \sin(2\omega t - 84.68^\circ) \text{ N} \quad (11)$$

$$z = 14.774 \sin(\omega t) + 2.248 \sin(2\omega t + 102.85^\circ) 10^{-6} \text{ m} \quad (12)$$

$$x = 3.813 \sin(\omega t - 6.63^\circ) 10^{-6} \text{ m} \quad (13)$$

$$\phi = 1.540 \sin(\omega t + 176.61^\circ) 10^{-3} \text{ rad} \quad (14)$$

Equations of Motion

The dynamic system is modeled as a three-degree-of-freedom system based on the experimental results. In Fig. 13, the coordinate z is in the normal direction, x is in the frictional direction and ϕ is the twist angle about the y axis. Considering the z axis, the total force in that direction is $F_{z0} + F_z$ where F_{z0} is the constant component and F_z is the dynamic component with zero mean value over a cycle. Letting F_{st} denote the applied normal load, k_z the arm stiffness, and k_{zc} the contact stiffness, as shown in Fig. 13, the steady state relationship is given by

$$F_{z0} = -k_{zc} z_0 = -k_z (z_M - z_0) = -F_{st} \quad (15)$$

where $-z_0$ is the slider penetration in the negative z -direction and $-z_M$ is the displacement of the massive block of mass M .

Neglecting the vibrations of the mass M , the equations of motion are written for the dynamic components only as

$$m\ddot{z} + c_z \dot{z} + k_z z = F_z \quad (16)$$

$$m\ddot{x} + c_x \dot{x} + k_x x = F_x \quad (17)$$

$$I\ddot{\phi} + c_t \dot{\phi} + k_t \phi = -LF_x \quad (18)$$

where L is the moment arm of force F_x about the y axis as shown in Fig. 13. The forces F_z and F_x can in general be functions of the steady state sliding speed, steady state normal load, displacements z, x and ϕ and their velocities.

Defining the natural frequencies and damping ratios as $\omega_z = k_z/m$, $\omega_x = k_x/m$, $\omega_t = k_t/I$, $2\zeta_z\omega_z = c_z/m$, $2\zeta_x\omega_x = c_x/m$, $2\zeta_t\omega_t = c_t/I$, we express (16) to (18) as

$$\ddot{z} + 2\zeta_z\omega_z\dot{z} + \omega_z^2 z = \frac{1}{m}F_z \quad (19)$$

$$\ddot{x} + 2\zeta_x\omega_x\dot{x} + \omega_x^2 x = \frac{1}{m}F_x \quad (20)$$

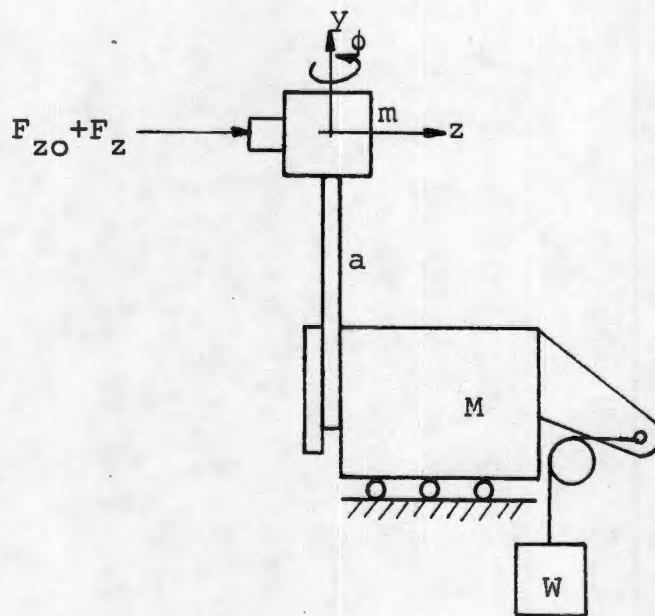
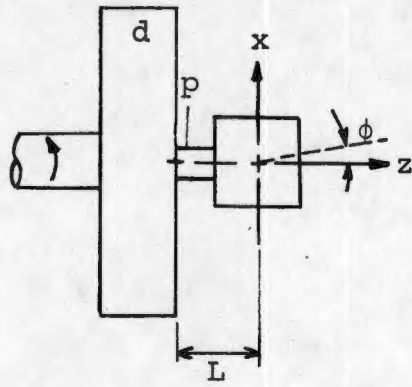
$$\ddot{\phi} + 2\zeta_t\omega_t\dot{\phi} + \omega_t^2 \phi = \frac{L}{I}F_x \quad (21)$$

The value of the vibrating mass is found to be $m = 2.48$ kg. The other parameter values are given by $I = k_t/\omega_x^2 = 3.147 \times 10^{-3}$ kg. m² and $L = 0.065$ m. Using these parameter values and the values of the natural frequencies (in radians) and damping ratios given previously, we obtain

$$\ddot{z} + 7.80\dot{z} + 119.422 \times 10^3 z = 0.403 F_z \quad (22)$$

$$\ddot{x} + 2.316\dot{x} + 93.823 \times 10^3 x = 0.403 F_x \quad (23)$$

$$\ddot{\phi} + 3.139\dot{\phi} + 384.976 \times 10^3 \phi = 20.655 F_x \quad (24)$$



d = disk
 p = pin
 m = oscillating mass
 M = inertial mass
 W = weight
 a = arm

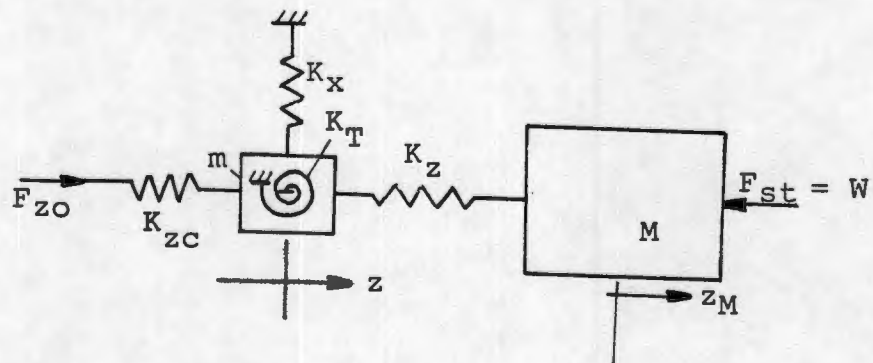


Fig. 13

Modeling of Contact Forces

A mathematical model of contact forces F_z and F_x is now obtained from the experimental data.

The normal contact force F_z is expressed as:

$$F_z = F_s + F_d + F_\phi$$

where F_s is the contact stiffness force, F_d is the contact damping force and F_ϕ is the normal force due to the twist angle ϕ .

In order to obtain the contact stiffness and contact damping in the normal direction the pin was placed in contact with the disk and loaded with different normal loads. The slider was hit impulsively in the normal direction and the natural frequencies and damping ratios were obtained for different values of the normal load, by employing a spectral analyzer. The results are given in the following table where the subscript zc refers to the natural frequency and damping ratio in the z -direction with pin in contact.

Table 1. Natural Frequencies and Damping in the normal direction

Normal load F_{z0} , N	Normal Frequency ω_{zc} , Hz	Damping Ratio ξ_{zc}
22.23	231.25	0.028
40.01	235.00	0.027
57.79	236.25	0.036
75.57	238.75	0.033
84.46	242.50	0.029
93.35	244.98	0.042

It is difficult to obtain an analytical model of the contact forces for this nonHerzian contact. Hence our approach is to obtain an empirical model based on the experimental data. Referring to equations (15) and Fig. 13 we have

$$K_{zC} + K_z = m\omega_{zC}^2$$

$$K_z = m\omega_z^2$$

Hence the contact stiffness is obtained from

$$K_{zC} = m(\omega_{zC}^2 - \omega_z^2)$$

$$= 2.48(2\pi)^2(\omega_{zC}^2 - (55)^2) \quad (25)$$

Since the contact stiffness is continuously varying with load or the slider penetration a quadratic function is chosen to represent the relationship between the contact stiffness force F_s and the slider penetration z , which is also in agreement with the wave forms of the normal force and the normal displacement obtained in the experimental results, where a second harmonic is observed.

$$F_s' = -K_s z' + K_a z'^2 \quad (26)$$

Where F_s' and z' are the total stiffness force and penetration measured from the disk surface.

Employing the values given in table (1) and using equations (25) and (26) and the relation:

$$K_{zC} = -\frac{dF_s'}{dz'}$$

we get $K_s' = 4.739 \times 10^6 \text{ N/m}$

and $K_a = 2.179 \times 10^{10} \text{ N/m}^2$

Then $F_s' = -4.739 \times 10^6 z' + 0.02179 \times 10^{12} z'^2$ which is plotted in Fig. 14.

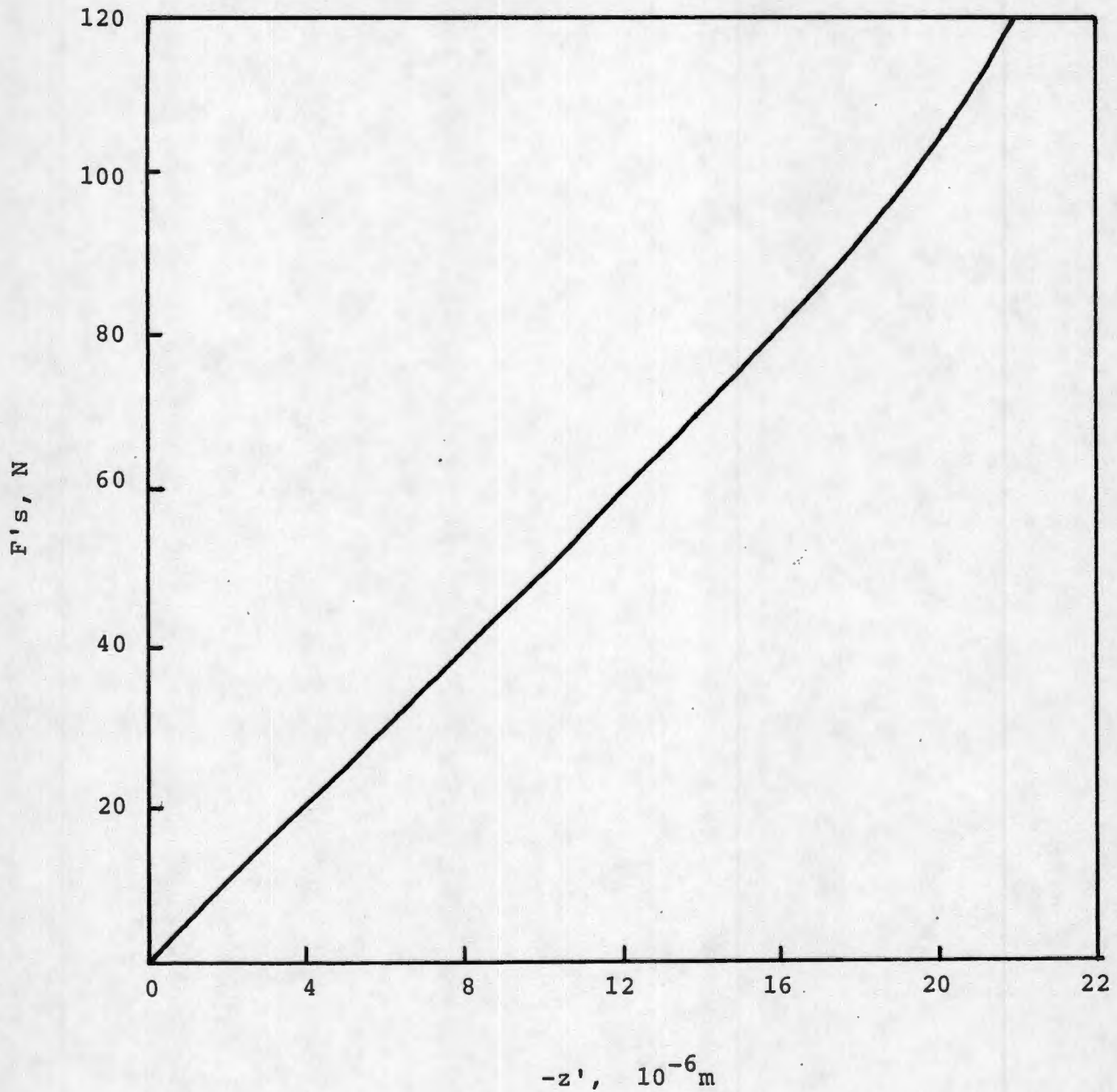


Fig. 14

Applying the last equation at the static load

$$F_{z0} = -4.739 \times 10^6 z_{st} + 0.02179 \times 10^{12} z_{st}^2$$

During the self excited vibration the static load F_{z0} was 84.46 N which yields $z_{st} = -16.561 \times 10^{-6} \text{ m}$. To get the relation between the dynamic parts of the stiffness force F_s and the penetration Z we have:

$$F_s = -5.461 \times 10^6 Z + 0.02179 \times 10^{12} Z^2 \quad (27)$$

where

$$F_s = F_s' - F_{z0}$$

$$Z = Z' - z_{st}$$

$$K_s = 5.461 \times 10^6$$

The coefficient of contact damping C_{zc} is given by

$$C_{zc} + C_z = 2m\xi_{zc} \omega_{zc}$$

$$C_z = 2m\xi_z \omega_z$$

then

$$\begin{aligned} C_{zc} &= 2m(\xi_{zc} - \xi_z \omega_z) \\ &= 2(2.48)(2\pi)(\xi_{zc}\omega_{zc} - 0.01129(55)) \end{aligned} \quad (28)$$

Table 2. Coefficient of contact damping and the normal load

Normal load F_{z0} , N	Contact Damping Coefficient C_{zc} , N.s/m
22.23	182.44
40.01	178.39
57.79	245.70
75.57	228.12
84.46	199.83
93.39	301.30

Since the contact damping coefficient does not show a specific change with the load, it was modeled as a constant

with an average value $C_{cz} = 222.63 \text{ N.s/m}$.

The force F_ϕ is the change in the contact force due to the twist angle ϕ , and that results from the curvature of the surface of the pin as wear takes place in one side more than the other.

Taking this force as a linear function in ϕ

$$\begin{aligned} F_\phi &= K_\phi \cdot \phi \\ F_\phi &= F_z - F_d - F_s \\ &= F_z + C_{zc} \dot{z} + K_s z - K_a z^2 \end{aligned}$$

By substituting the values of F_z , \dot{z} , and z from equations (2), (4), (6), and (8) at different points in the cycle and averaging over one cycle we get a value of $K_\phi = -47.64 \cdot 10^3 \text{ N/rad}$.

The wave forms of the contact forces as shown in Fig. 12 and as represented by equations (10) and (11), show that both the normal contact force F_z and the friction force F_x have two harmonics, the fundamental and the second harmonic, and they also indicated that the one harmonic in one force corresponds in phase angle with the same harmonic in the other, but the ratio of the second harmonic to the fundamental harmonic is higher in F_x than in F_z .

Representing F_x as:

$$F_x = \mu F_z$$

where μ is the coefficient of friction, and using the ratio of the fundamental harmonics we get $\mu = 0.215$.

Solution of the System Equations

The system equations of motion as mentioned before are summarized here:

$$\frac{F_z}{m} = \ddot{z} + 2\xi_z \omega_z \dot{z} + \omega_z^2 z \quad (29)$$

$$\frac{F_x}{m} = \ddot{x} + 2\xi_x \omega_x \dot{x} + \omega_x^2 x \quad (30)$$

$$-\frac{F_x}{I} \cdot L = \ddot{\phi} + 2\xi_T \omega_T \dot{\phi} + \omega_T^2 \phi \quad (31)$$

The contact forces are given as:

$$F_z = -K_s z + K_a z^2 - C_{zc} \dot{z} + K_\phi \cdot \phi \quad (32)$$

$$F_x = \mu F_z \quad (33)$$

From the above equations the two degrees of freedom z and ϕ are coupled and the asymmetric term $K_a z^2$ will give rise to a second harmonic in z in addition to a constant term

$$z = z_0 + z_1 + z_2$$

where z_0 is the average of z

z_1 is the fundamental harmonic

z_2 is the second harmonic

Also, $\phi = \phi_1 + \phi_2$

Employing the frequency domain to solve the system equations, the nonlinear term is substituted by its describing function. In order to get this describing function a triple input is used as:

$$z = A_0 + A_1 \sin(\psi + \theta_1) + A_2 \sin(2\psi + \theta_2)$$

where $A_0 = z_0$

$$A_1 = |z_1|$$

$$A_2 = |z_2|$$

$$\theta_1 = \text{phase angle of } z_1$$

$$\theta_2 = \text{phase angle of } z_2$$

$$\psi = \omega t$$

Fig. 15 shows this input to the nonlinearity and N_0 , N_1 , and N_2 are the describing functions of the constant term, the fundamental and the second harmonic respectively, and y is the nonlinearity output.

Analyzing y into its harmonics in terms of A_0 , A_1 , A_2 , ψ , θ_1 , and θ_2 , and neglecting the harmonics higher than the second, and using the definition

$$\text{Describing Function} = \frac{\text{phasor representation of output component at frequency } \omega}{\text{phasor representation of input component at frequency } \omega}$$

we get

$$N_0 = K_a \left(A_0 + \frac{1}{2A_0} (A_1^2 + A_2^2) \right)$$

$$N_1 = K_a [(2A_0 - A_2 \sin\theta) + jA_2 \cos\theta]$$

$$N_2 = K_a \left[(2A_0 - \frac{A_1^2}{2A_2} \sin\theta) - j\frac{A_1^2}{2A_0} \cos\theta \right]$$

where

$$\theta = \theta_2 - 2\theta_1$$

= relative phase angle between the second and the fundamental harmonics of z

Converting the equations (29), (30), and (31) into frequency domain:

$$\frac{F_{z1}}{m} = L_{z1} (j\omega) z_1 \tag{34}$$

$$\frac{F_{z2}}{m} = L_{z2} (2j\omega) z_2 \tag{35}$$

$$\frac{F_{x1}}{m} = L_x (j\omega) x \tag{36}$$

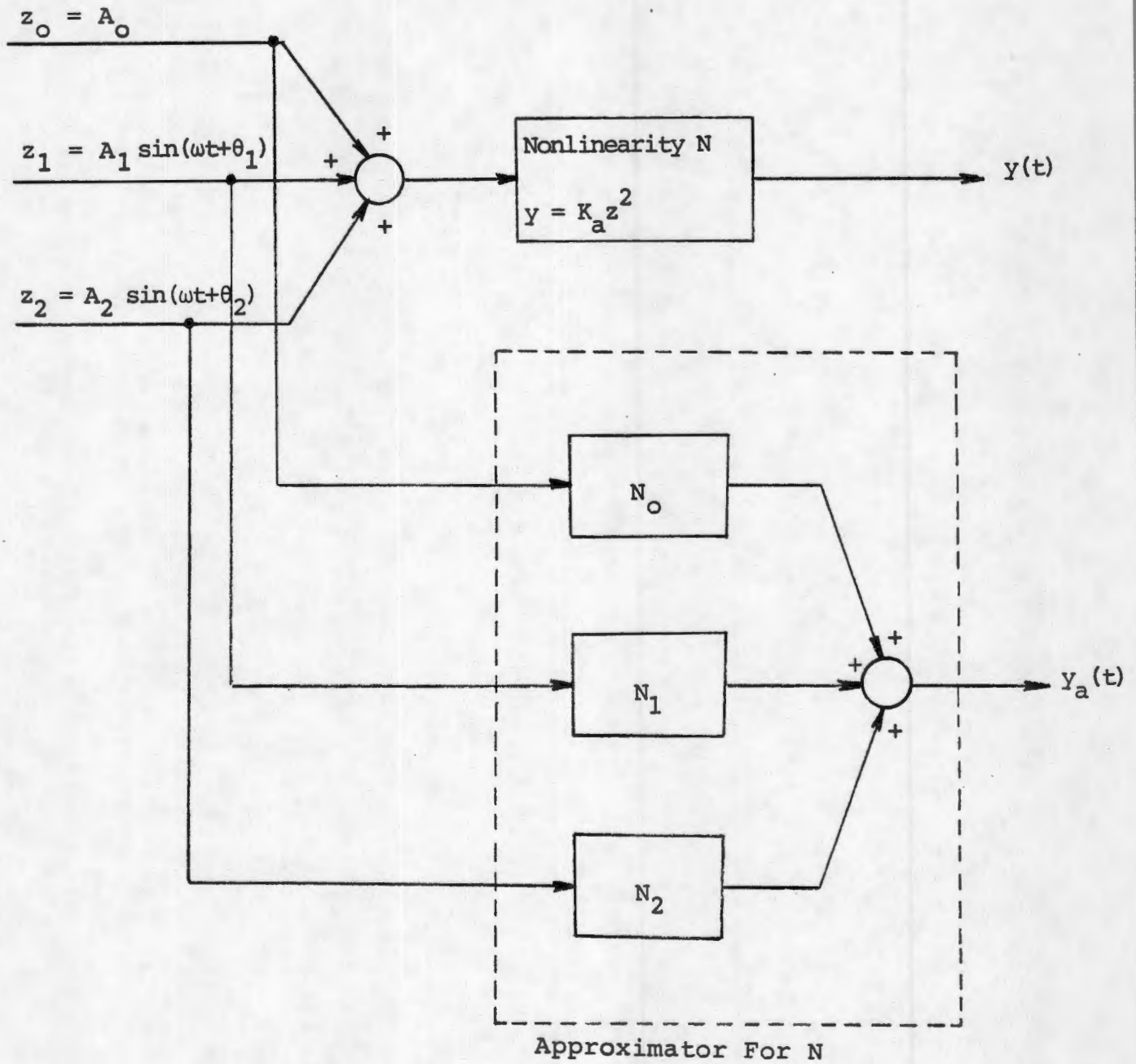


Fig. 15

$$- \frac{F_{x1}}{I} \cdot L = L_{T1} (j\omega) \phi_1 \quad (37)$$

$$- \frac{F_{x2}}{I} \cdot L = L_{T2} (2j\omega) \phi_2 \quad (38)$$

where

$$L_{z1} (j\omega) = -\omega^2 + \omega_z^2 + 2j\xi_z \omega_z \omega$$

$$L_{z2} (2j\omega) = -4\omega^2 + \omega_z^2 + 4j\xi_z \omega_z \omega$$

$$L_x (j\omega) = -\omega^2 + \omega_x^2 + 2j\xi_x \omega_x \omega$$

$$L_{T1} (j\omega) = -\omega^2 + \omega_T^2 + 2j\xi_T \omega_T \omega$$

$$L_{T2} (2j\omega) = -4\omega^2 + \omega_T^2 + 4j\xi_T \omega_T \omega$$

Using equations (32) and (33) to eliminate F_x and F_z in equations (34) through (38) and using the describing functions in place of the nonlinear term:

$$L_{z1} (j\omega) z_1 = -K_s z_1 + N_1 z_1 - j\omega \frac{C_{zc}}{m} z_1 + K_\phi \phi_1 \quad (39)$$

$$L_{z2} (2j\omega) z_2 = -K_s z_2 + N_2 z_2 - 2j\omega \frac{C_{zc}}{m} z_2 + K_\phi \phi_2 \quad (40)$$

$$L_{T1} (j\omega) \phi_1 = -\frac{\mu L m}{I} L_{z1} (j\omega) z_1 \quad (41)$$

$$L_{T2} (2j\omega) \phi_2 = -\frac{\mu L m}{I} L_{z2} (2j\omega) z_2 \quad (42)$$

$$L_x (j\omega) x = -\mu L_{z1} (j\omega) z_1 \quad (43)$$

Solving equations (39) to (42) in z_1 and z_2 we get

$$\begin{aligned} & L_{z1} (j\omega) \left(1 + \frac{\mu L m}{I} K_\phi / L_{T1} (j\omega)\right) + K_s + j\omega \frac{C_{zc}}{m} \\ &= K_a [(2A_o - A_2 \sin\theta) + jA_2 \cos\theta] \end{aligned} \quad (44)$$

$$\begin{aligned} & L_{z2} (2j\omega) \left(1 + \frac{\mu L m}{I} K_\phi / L_{T2} (2j\omega)\right) + K_s + 2j\omega \frac{C_{zc}}{m} \\ &= K_a \left[(2A_o - \frac{A_1^2}{2A_2} \sin\theta) - j \frac{A_1^2}{2A_o} \cos\theta\right] \end{aligned} \quad (45)$$

Also we have the equation of equilibrium for z_0 :

$$-K_s + K_a \left[A_0 + \frac{1}{2A_0} (A_1^2 + A_2^2) \right] = 0 \quad (46)$$

and
$$\phi_1 = \frac{\mu L_m}{I} \frac{L_{z1}(j)}{L_{T1}(j)} A_1 \quad (47)$$

$$\phi_2 = -\frac{\mu L_m}{I} \frac{L_{z2}(2j\omega)}{L_{T2}(2j\omega)} A_2 \quad (48)$$

$$x = -\mu \frac{L_{z1}(j\omega)}{L_x(j\omega)} A_1 \quad (49)$$

Equations (44) to (49) are nonlinear algebraic equations in ω , A_0 , A_1 , A_2 , θ , ϕ_1 , ϕ_2 , and x with ϕ_1 , ϕ_2 , and x are complex variables consisting of amplitudes and phase angles relative to the fundamental harmonic z_1 .

The system parameters as found before were substituted in these equations, and a computer program was written to solve them using the grid method, and the solution yielded:

$$\omega = 647.034 \text{ rad/s}$$

$$z = 14.460 \sin \omega t + 2.289 \sin(2\omega t + 253.31^\circ) + 0.42 \cdot 10^{-6} \text{ m}$$

$$\phi = 1.413 \sin(\omega t + 180.21^\circ) \cdot 10^{-3} \text{ rad}$$

$$x = 2.864 \sin(\omega t - 0.70^\circ) \cdot 10^{-6} \text{ m}$$

Equation (44) and (45) can be written as

$$L_1(\omega) = NL_1(A_0, A_1, A_2, \theta)$$

$$L_2(\omega) = NL_2(A_0, A_1, A_2, \theta)$$

In Fig. 16 and Fig. 17, the solution points of the system equations are shown as the intersection point of the curves representing the linear parts $L_1(\omega)$ and $L_2(\omega)$ with the curves representing the nonlinear parts $NL_1(A_1)$ and $NL_2(A_2)$.

Comparing these results with the experimental results

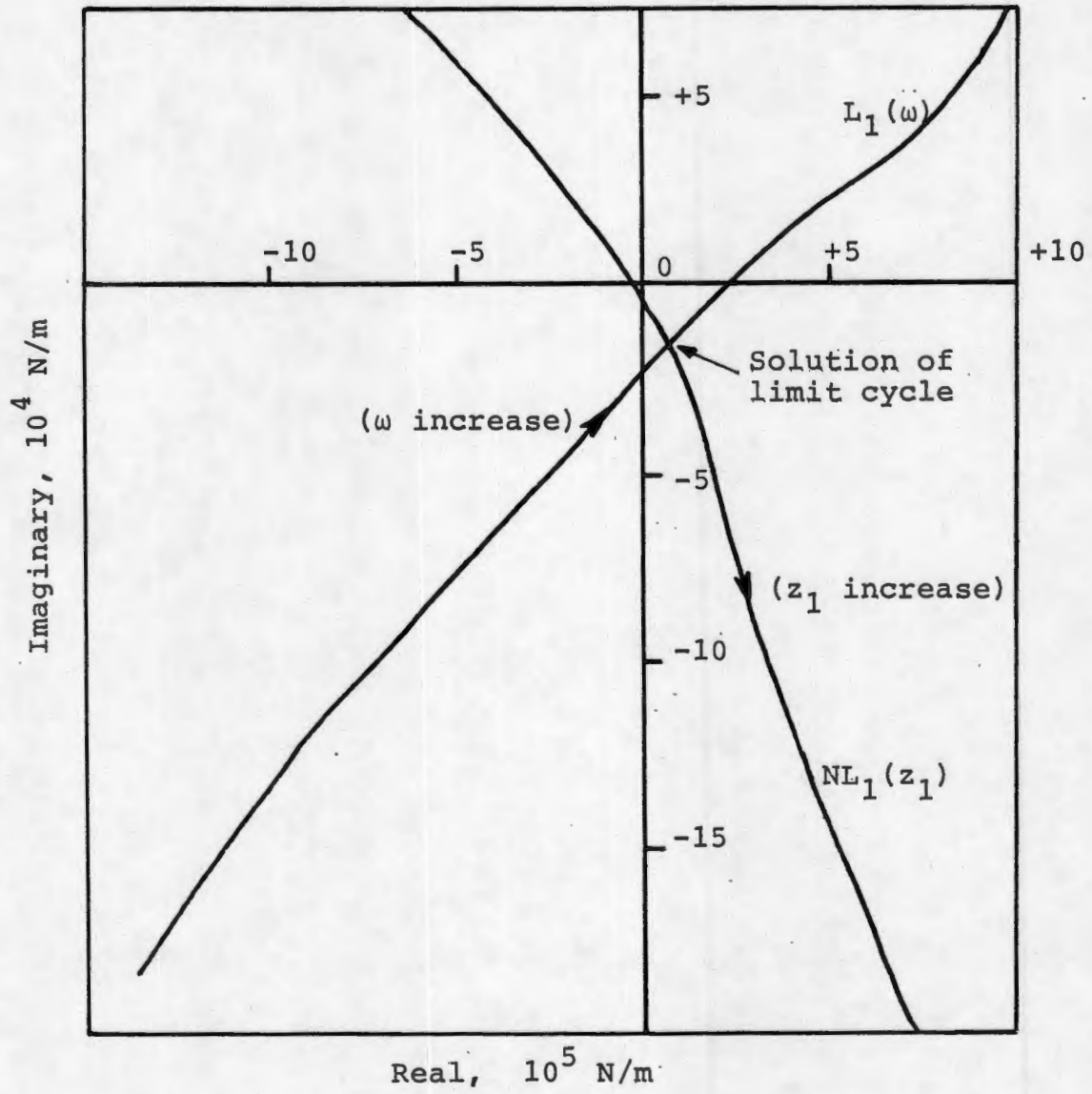


Fig. 16

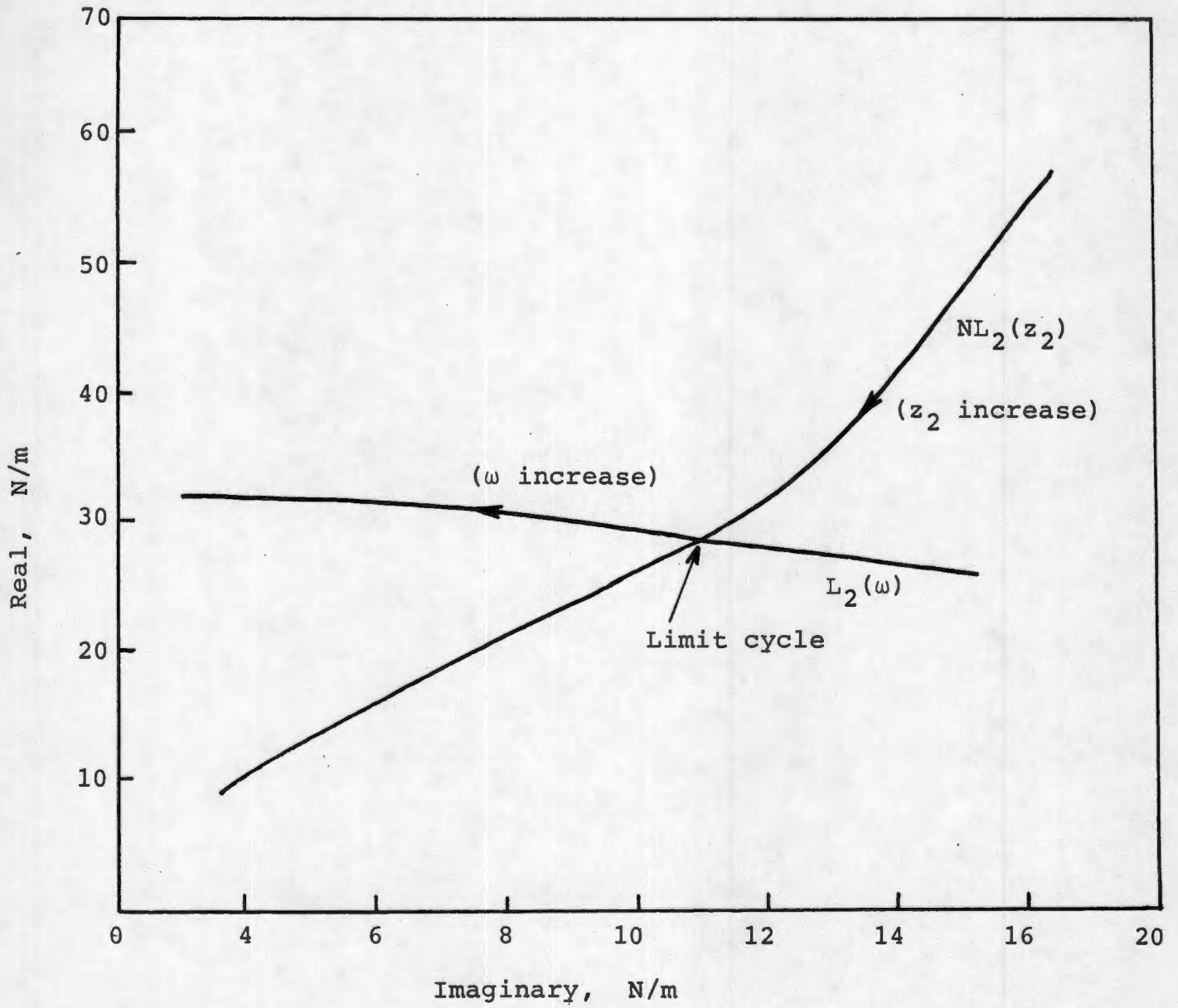


Fig. 17

obtained for the displacements and frequency ν during the self-excited vibration, equations (12), (13), and (14), it is found that except for the phase angle of the second harmonic of the normal displacement, they are generally in agreement.

V SUMMARY AND CONCLUSIONS

The interactions among friction, wear, and system dynamics have been investigated for dry sliding contact between two metallic surfaces, one cast iron and the other steel. The experimental results, using a pin-on-disk setup instrumented with force and acceleration transducers, reveal that as the normal load is increased, four different regimes are encountered in sliding of steel on a cast iron surface without lubrication.

The steady state friction regime is characterized by a coefficient of friction that is independent of normal load, small rate of wear (mild wear), absence of surface damage, smoothing of the surface, and small amplitude of slider oscillations. The second regime is the region of nonlinear friction characterized by coefficient of friction that increases with normal load, large rate of wear (severe wear), increase in the amplitude of slider oscillations with normal load and increase in surface roughness.

The third regime is the region of transient friction where the friction force varies with time for a constant normal load so that a coefficient of friction cannot be defined and there are self-disturbances that cause a sharp increase and decrease of the friction force. This is a region of severe wear and surface damage. The last regime is the region of self-excited vibrations characterized by

periodic oscillations of the slider and a wear rate several orders of magnitude higher than that observed in any other region.

The transition from mild to severe wear corresponds to the transition from steady state friction regime to the nonlinear friction region. The range of the region of steady state friction can be increased by increasing the system stiffness for unlubricated contact. A model is developed for mild wear in the region of steady state friction including the effect of slider oscillations in the normal direction. It is shown that wear is an increasing function of system stiffness.

The experimental setup was modified for further detailed study of self-excited oscillations. A non-interaction dynamometer was constructed to hold the slider. It is instrumented with strain gages and tri-axial accelerometer to provide accurate measurements of they dynamic contact forces and displacements in different directions, in addition to the static components of the forces.

The experimentally recorded waveforms show that the oscillations are periodic but not simple harmonic. A decomposition of the waveforms into Fourier Series indicated that the waveforms of the force components and of the displacement in the normal direction contain a fundamental frequency and its second harmonic component

which is a result of nonlinearity.

A mathematical model is developed to analyze the self-excited oscillations. The model has three degrees of freedom and includes the coupling among the different degrees of freedom and the nonlinearity of the contact stiffness. The contact stiffness and damping as well as the other parameter values of the model were identified experimentally under free vibration conditions. The study showed that the contact stiffness is an asymmetric nonlinear function of the slider penetration.

The nonlinear mathematical model was analyzed by the method of triple input describing functions to include the constant, fundamental and second harmonic components. The results of the analysis are generally in agreement with the experimental observations regarding the frequencies and amplitudes of the oscillations. The fundamental frequency of oscillations is nearly equal to the natural frequency of the system in the torsional direction. The effect of the coupling between the normal and torsional degrees of freedom is found to be important for the existence of self-excited oscillations.

Acknowledgments

This study was sponsored by the U.S. Department of Energy under contract No. DE-AC02-82ER12071 on "Interactions Between Friction-Induced Vibration and Wear." We would like to extend our thanks to Dr. Oscar P. Manley of the Division of Engineering, Mathematical and Geosciences for his support of this project.

REFERENCES

1. Soom, A., and Kim, C., "Roughness-Induced Dynamic Loading at Dry and Boundary-Lubricated Sliding Contacts", ASME Journal of Lubrication Technology, October 1984, pp. 514-517.
2. Ko, P.L., and Brockley, C.A., "The Measurement of Friction and Friction-Induced Vibration", ASME Journal of Lubrication Technology, October 1970, pp. 543-549.
3. Krauter, A.I., "Generation of Squeal/Chatter in Water-Lubricated Elastometric Bearings", ASME Journal of Lubrication Technology, July 1981, pp. 406-413.
4. Earles, S.W.E., and Lee, C.K., "Instabilities Arising from the Frictional Interaction of a Pin-Disk System Resulting in Noise Generation", ASME Journal of Engineering for Industry, Feb. 1976, pp. 81-86.
5. Aronov, V., D'Souza, A.F., Kalpakjian, S., and Shareef, I., "Experimental Investigation of the Effect of System Rigidity on Wear and Friction-Induced Vibrations", ASME Journal of Lubrication Technology, April 1983, pp. 206-211.
6. Aronov, V., D'Souza, A.F., Kalpakjian, S., and Shareef, I., "Interactions Among Friction, Wear and System Stiffness - Part I: Effects of Normal Load and System Stiffness", ASME Journal of Tribology, January 1984, pp. 54-58.
7. Aronov, V., D'Souza, A.F., Kalpakjian, S., and Shareef, I., "Interactions Among Friction, Wear and System Stiffness - Part 2: Vibrations Induced by Dry Friction", ASME Journal of Tribology, January 1984, pp. 59-64.
8. Aronov, V., D'Souza, A.F., Kalpakjian, S., and Shareef, I., "Interactions Among Friction, Wear and System Stiffness - Part 3: Wear Model", ASME Journal of Tribology, January 1984, pp. 65-69.
9. Zaprogetz, V., "Friction and Wear Investigations by Spectrum Analysis", Friction, Lubrication and Wear of Machine Elements, Vol. 5, 1969.
10. Zaprogetz, V., "Friction Force Oscillation", UCXA, Vol. 51, 1970.
11. Rice, S.L., Nowotny, H. and Wayne, S. F., "The Role of Specimen Stiffness in Sliding and Impact Wear", Wear, Vol. 77, 1982, pp. 13-28.
12. Kato, K., Iwabuchi, A., and Kayaba, T., "The Effect of Friction Induced Vibration on Friction and Wear", Wear, Vol. 80, 1982, pp. 307-320.

13. Miyagawa, Y., Seki, K., and Nishimura, T., J. Jpn. Soc. Lubr. Engg., Vol. 18, 1973, pp. 323, (in Japanese).
14. Tolstoi, M., "Significance of the Normal Degree of Freedom and Natural Normal Vibrations in Contact Friction", Wear, Vol. 10, 1967, pp. 199-213.
15. Broszeit, E., Kloos, K.H., Hess, F.J. and Wagner, E., "Influence of Vibrations on the Wear Properties on a Tribological System", Wear, Vol. 28, 1974, pp. 395-401.
16. Elder, J.A. and Eiss, N.S., "A Study of the Effect of Normal Stiffness on Kinetic Friction Forces Between Two Bodies in Sliding Contact", ASME Journal of Lubrication Technology, 1969, pp. 234-241.
17. Budanov, B.V., Kudinov, V.A. and Tolstoi, D.M., "Interaction of Friction and Vibrations", Trenieilznos, Vol. 1, 1980, pp. 79-89 (Russian).
18. Soda, N., Kimura, Y. and Tanaka, A., "Wear of Some f.c.c. Metals During Unlubricated Sliding. Part 1: Effects of Load, Velocity and Atmosphere Pressure on Wear" Wear, Vol. 33, 1975, pp. 1-16.
19. Gelb, A. and Vander Velde, W.E., Multiple-Input Describing Functions and Nonlinear System Design, McGraw Hill Book Company, New York, 1968.

APPENDIX 1



ASME

THE AMERICAN SOCIETY OF MECHANICAL ENGINEERS
345 E 47 St., New York, N.Y. 10017

The Society shall not be responsible for statements or opinions advanced in papers or in discussion at meetings of the Society or of its Divisions or Sections, or printed in its publications. Discussion is printed only if the paper is published in an ASME Journal or Proceedings. Released for general publication upon presentation. Full credit should be given to ASME, the Technical Division, and the author(s).

V. Aronov

A. F. D'Souza

S. Kalpakjian

I. Shareef

Department of Mechanics and
Mechanical and Aerospace Engineering,
Illinois Institute of Technology,
Chicago, Ill. 60616

Experimental Investigation of the Effect of System Rigidity on Wear and Friction-Induced Vibrations

This paper presents experimental data and a physical model of the effects of normal load and system rigidity on the friction and wear processes with water lubrication. The transition from mild to severe friction and wear was found to be independent of the system rigidity, but dependent on the normal load. As the normal load is increased further, it reaches another critical value, which depends on the system rigidity, at which high frequency self-excited vibrations are generated. These oscillations exhibit a coupling between the frictional and normal degrees of freedom. It is shown that mild wear rate increases with the normal load and also with the system rigidity.

Introduction

Several different types of friction-induced vibrations have been reported in the literature. It is apparent that there exist several distinct mechanisms that can excite these different types of oscillations. Self-excited vibrations of the stick-slip type have been studied by several investigators in the past [1]. They occur at very low sliding speeds and, as observed by Ko and Brockley [2], have almost a sawtooth waveform. As discussed by Brockley, Cameron, and Potter [3], the mechanism that causes stick-slip is attributed to the fact that there is a difference between the static and kinematic coefficients of friction and static friction is a time-varying function as it usually increases with time. The time-dependence of static friction is discussed by Brockley and Davis [4]. As the sliding speed is increased, there exists a critical value of the speed above which stick-slip type of vibrations do not occur [3].

In the study of Brockley and Ko [5], as the sliding speed was increased further, it was observed that there exists another critical speed at which a different type of self-excited vibrations are induced. They attribute the mechanism that excites these vibrations (called quasi-harmonic) to the negative slope of the friction versus sliding speed curve which feeds the energy to the vibrating system. Yokoi and Nakai [6] also observed quasi-harmonic vibrations which they named "squeal." These vibrations occurred not only in the region where the slope of the friction force versus sliding speed is negative, but also in the region where it is positive. They state that their experimental results are inconsistent with the belief that self-excited vibrations are not generated when the slope of the friction force versus sliding speed is positive.

Bhushan [7] employed a glass slider, sliding over a rubber

stave with water lubrication. He observed two types of friction induced vibrations, namely, low frequency oscillations which he has named "chatter" and high frequency oscillations which he has named "squeal." Generally, squeal was generated at low normal loads and high speeds, whereas chatter was generated at high load and low speed or very high load and any speed. Krauter [8] has presented a three-deg-of-freedom linear mathematical model to predict the onset of squeal/chatter instabilities.

Usually it can be expected that any type of friction induced vibrations will cause damage to the surface and result in excessive wear. In other words, the onset of friction induced oscillations may cause transition from mild to severe wear. Under sliding conditions, wear of metals is characterized by two modes, called mild and severe wear; this has been recognized for many material combinations and by many investigators [9-11]. Hence it is very important to study these interactions and their effects.

This paper presents some experimental results of an investigation that is in progress to study the interaction between friction, wear, and system rigidity, including self-excited oscillations. The results reported here pertain to a metal pin sliding on a rotating metal disk under the action of water as a lubricant. In this phase of the study, the normal load was varied and the sliding speed was kept constant at 73 cm/s which is sufficiently high so that vibrations of the stick-slip type do not occur.

Experimental Techniques

(a) **Test Apparatus.** A schematic of the test apparatus is shown in Fig. 1. The design consists of measuring and loading systems.

The loading system can move linearly in a single direction perpendicular to the disk. It primarily consists of a massive block (3) pulled over the antifriction linear bearings (4) by virtue of a dead weight (1) and a rope and a pulley system (2). The massive block is damped by a damper (5) (using a viscous oil) at the bottom and incorporates an adjustable clamping

Contributed by the Lubrication Division of THE AMERICAN SOCIETY OF MECHANICAL ENGINEERS for presentation at the ASLE-ASME Joint Lubrication Conference, New Orleans, La., October 4-7, 1981, New Orleans, La. Manuscript received by the Lubrication Division, February 19, 1981. Paper No. 81-Lub-3.

Copies will be available until June, 1982.

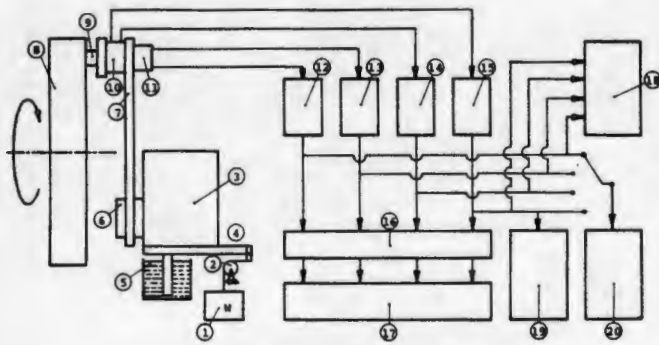


Fig. 1 Schematic of test apparatus

system (6) in the front. The stiffness of the spring can be altered by changing the distance between the clamps and the sample (9), as well as changing the cross-section of the spring. In this phase of the study, the cross-section of the spring was kept constant (1.25×1.25 cm).

The measuring system consists of a spring (7), flexible in frictional (tangential to disk (8)) and normal (normal to the disc) directions. The load cell (10) is placed between the sample and the spring (7) by means of an expansion bolt, whose other end holds the accelerometer (11). The preamplifiers (12) and (13) are comprehensively equipped, charge conditioning amplifiers intended to take input charge from piezoelectric accelerometer to give an output in the form of acceleration. The device incorporates built-in double integrators which provide velocity and displacement outputs. The preamplifiers (14) and (15) take the input charge from the piezoelectric load cell. The charge outputs from the load cell and accelerometer in frictional and normal directions are connected to preamplifiers (15)-(13) and (14)-(12), respectively. The outputs from the preamplifiers are connected to (i) four channel visicorder (17) via the main amplifier (16), (ii) dual trace storage oscilloscope (18), (iii) strip chart recorder (19), and (iv) micro FFT analyzer (20).

The resolution of the triaxial force transducer is 0.01 N (0.0022 lb) and its resonant frequency is about 8 KHz. The cross influence is less than 5 percent and the linearity is within 1 percent. Due to the high rigidity of the force transducer, its influence on the measurements is negligible. The frequency range of the triaxial accelerometer is from 1 Hz to 10 KHz and the maximum cross sensitivities are 0.4, 2.0 and 2.4 percent in the z , x , and y direction, respectively.

(b) Materials and Lubrication. The materials were selected in such a way as to investigate the process of mild wear and the processes of transition from mild to severe wear, both in dry and boundary lubrication regimes. RY-ALLOY, an oil hardening AISI-SAE 01 steel consisting of 0.9 percent C, 0.5 percent Cr, 1.35 percent Mn, 0.5 percent W, and 0.35 percent Si, was chosen for disk material which was subsequently oil hardened to 59 Rockwell C. A special quality 1045 steel consisting of 0.5 percent C, 0.85 percent Mn, 0.04 percent P, and 0.05 percent S, was hardened to 45 Rockwell C to be used as the pin material.

Preliminary experiments with dry friction showed that there was a small range of speeds and loads at which steady state friction and mild wear can be achieved. In order to increase this range, lubrication was introduced. As a lubricant, ordinary tap water was used because of its low viscosity which, together with flat on flat contact geometry and low sliding speed (73 cm/s), is not expected to cause hydrodynamic lubrication.

(c) Testing Technique. In order to investigate the effect of system rigidity on the transition from mild to severe wear, four different arm lengths 3.18 cm (1.25 in.), 6.76 cm (2.66

in.), 10.19 cm (4.01 in.), and 13.97 cm (5.5 in.) corresponding to stiffnesses K_1 , K_2 , K_3 , and K_4 , respectively, were chosen. The arm was clamped at any one of these four lengths. The natural frequencies in the normal and frictional directions corresponding to the four stiffnesses K_1 , K_2 , K_3 , and K_4 were obtained with the disk not rotating and for both cases of the pin in contact with the disk and not in contact with the disk.

The pin was hit impulsively by a force in the normal and frictional directions, respectively. The spectra of the impulse responses of the accelerometer in both the normal and frictional directions were analyzed by the Fourier analyzer and also observed on the storage oscilloscope. The values of the natural frequencies and damping ratio are given later in the next section.

The pin (1.10 cm (0.435 in.) dia) and the disk were lapped in situ to a smooth finish ($0.42 \mu\text{m}$ CLA) under a normal load of 9 N (2 lb). After cleaning and introducing water drops, the pin was brought in contact with the rotating disk under a normal load of 9 N (2 lb). The disk rpm was set at 76 rpm in all the experiments corresponding to a sliding speed of 73 cm/s. Under this condition, extremely smooth and stable friction process was achieved. This state was continued for 10 hr in order to doubly make sure that full contact of the pin surface has been achieved. After achieving this, the load was applied in steps of 9 N (2 lb) and at intervals of 40 min. In between each load, the friction force (F_x), normal force (F_z), frictional velocity (V_x), normal velocity (V_z), and their corresponding spectra were recorded on a Visicorder chart. A trace of the friction force variation on a strip chart recorder was also obtained.

Wear experiments were carried out on the same pin-on-disk setup. The pin diameter was 1.1 cm (0.435 in.) with a flat wear surface. In the beginning of each experiment, the pin and disk were lapped with 600 grit size clover lapping compound and were subsequently cleaned thoroughly by methanol and acetone. Taking all precautionary steps, the pin and disk were brought in contact and maintained for a sufficiently long time (usually 4-6 hr) to insure full contact of the pin surface. The pin was then removed, weighed accurately (up to five decimal places of a gram) and replaced back in the same position. After wearing out the pin over a sliding distance of 15,000-16,000 m, the pin was reweighed and the difference taken as weight loss.

In all experiments, the disk surface speed was maintained at 73 cm/s and water was introduced as a lubricant at the rate of one drop/s on the disk track approximately 1 cm ahead of the pin-disk contact. Water lubrication readily provided boundary lubrication which resulted in desired higher wear rates. Wear data was obtained for spring stiffnesses K_1 , K_3 , and K_4 where $K_1 > K_3 > K_4$.

Natural Frequencies of Pin and Arm. The natural frequencies of the pin and arm were determined experimentally, as discussed in the previous section, in order to investigate the relationships, if any, between the low and high frequency self-excited oscillations and the natural frequencies. For each arm length, it was found that the natural frequencies when the pin is in contact with the disk are different from those when the pin is not in contact. Also, the natural frequencies when the pin is in contact with the disk do not depend on the normal load. The natural frequencies are given in Table 1. As expected, there also exist higher harmonics, but only the fundamental frequencies are shown in Table 1.

In order to obtain the damping ratios experimentally, the impulse responses of the accelerometer in both the normal and frictional directions were displayed in the time domain on the storage oscilloscope. By employing the method of logarithmic decrement, it was found that the dimensionless damping ratio ζ is approximately the same in both the normal

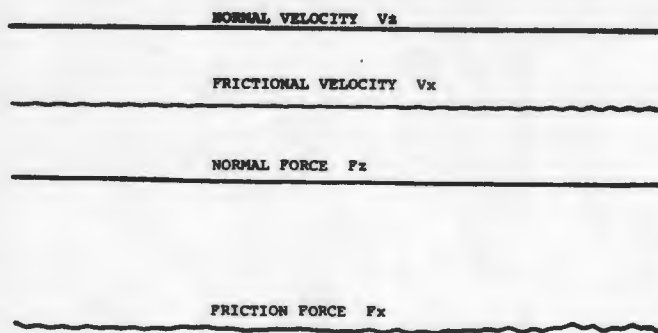


Fig. 2 Steady-state friction process

and frictional directions for all four stiffnesses tested. This value is given approximately by $\zeta = 0.02$.

Table 1 Natural frequencies

Stiffness	Pin in contact with disk		Pin not in contact with disk	
	Normal direction Hz	Frictional direction Hz	Normal direction Hz	Frictional direction Hz
K_1	1050	1050	915	815
K_2	575	575	410	420
K_3	435	435	240	250
K_4	355	355	165	170

Experimental Results

As the normal load was increased, with the disk rotating at the constant speed of 76 rpm, three different regions of operation were characterized by the behavior of the friction force F_x , the normal force F_z , the pin velocity components V_x , V_z , the nature of pin surfaces as examined under scanning electron microscope, and the wear rate measured as weight loss per unit sliding distance.

(a) Region of Stable, Steady-State Friction. When the normal load is low and below a certain critical value, the steady state friction process is stable with small fluctuations of the two force components and the two pin velocity components as shown in Fig. 2. The scanning electron microscope (SEM) photos of the pin surface are given in Fig. 3. The pin surface, after lapping and before starting the experiment, is shown in Fig. 3(a). At this stage, the surface is uniform with a roughness of $0.42 \mu\text{m CLA}$.

A SEM photo of the pin surface after 10 hr of operation in the region of steady-state friction with a normal load of 9 N (2 lb) is shown in Fig. 3(b). Here, the surface appears to be smooth, without any significant damage, covered with oxide film. In this region, the wear is mild or oxidative wear.

The variation of the wear rate with normal load is shown in Fig. 4 for three values of the stiffnesses. In this region of steady-state friction process, the mild wear rate is seen to increase with the normal load and also with the system rigidity. The increase in the mild wear rate with the increase in the square of the natural frequency, which is a measure of the system rigidity, is also shown in Fig. 5 for a normal load of 9 N (2 lb). Although the wear rate increases with the increase in rigidity, it appears that after a certain stage, the increase in wear rate saturates with increasing rigidity.

(b) Region of Intermittent Self Disturbances. As the normal load is increased beyond a certain critical value, which in this

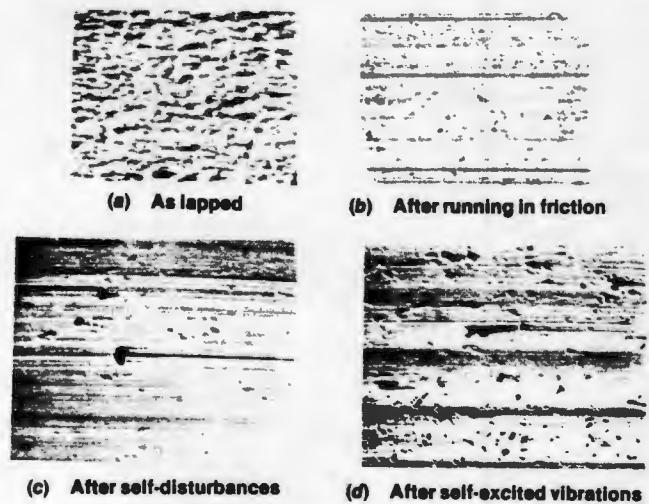


Fig. 3 S.E.M. photos of pin surface

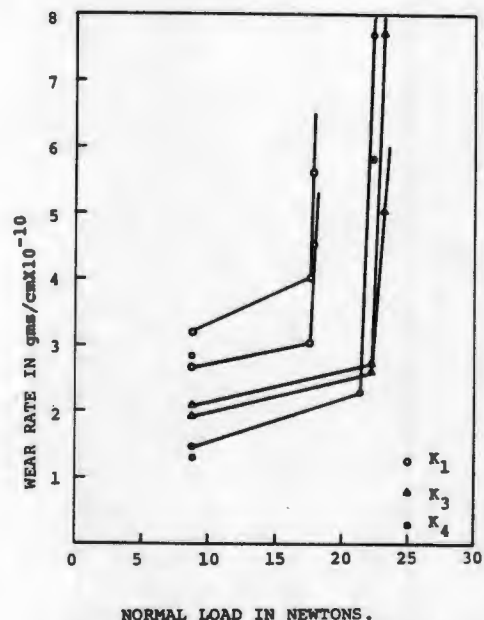


Fig. 4 Wear rate versus normal load

case is about 18–27 N (4–6 lb), a transition occurs from a steady-state friction process to an unstable process, characterized by the appearance of self-disturbances. During a disturbance, the friction force suddenly increases from its nominal value and decreases back to it, as seen in Fig. 6. Oscillations of two different frequencies can be observed in this figure.

The low frequency oscillations appear as soon as the friction force begins to increase from its nominal value. When the friction force has reached its high value, additional high frequency oscillations begin to appear. These high frequency oscillations decay quickly and disappear soon after the friction force decreases back to its nominal value. The low frequency oscillations, however, decay at a much slower rate. In case the time interval between two successive disturbances is sufficiently large, the low frequency oscillations also disappear and a comparatively smooth friction process reoccurs between the disturbances. At this state of friction, the two forces and two velocity components appear to be similar to the one shown in Fig. 2.

However, when the time interval between two successive disturbances is small, the low frequency oscillations do not have sufficient time to decay and they persist between the

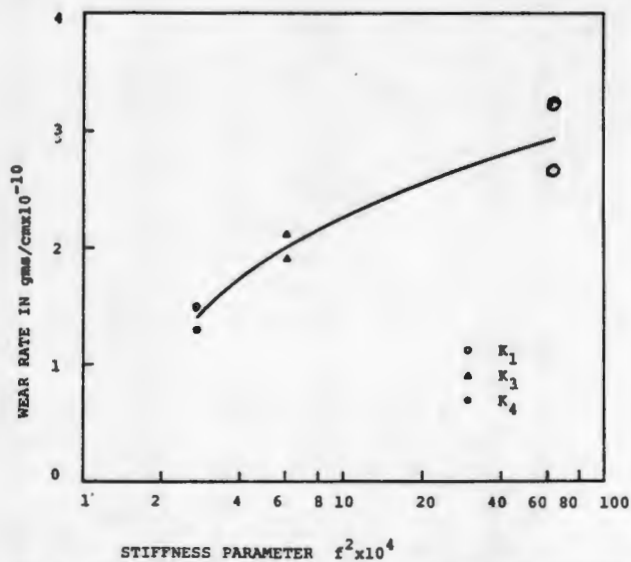


Fig. 5 Wear rate at 9 N normal load versus stiffness parameter f^2 (squared natural frequency)

disturbances. Both the low frequency and high frequency oscillations have been observed in the published literature [7]. As mentioned earlier, the low frequency oscillation has been named chatter and the high frequency has been named squeal. Both the low and high frequencies depend on the system rigidity and increase as the stiffness is increased. In Fig. 6, which is for stiffness K_3 corresponding to the arm length of 10.19 cm (4.01 in.), the lower frequency has the value of 240 Hz and the higher, 889 Hz. It is seen from Fig. 6 that the coupling between the frictional and normal degrees of freedom exists only for the higher frequency oscillations. The lower frequency oscillations occur only in the frictional direction.

The number of self-disturbances occurring during a time interval was also recorded on a strip chart recorder. The frequency of occurrence of disturbances would be high soon after a change in the normal load. As the elapsed time from a change in the normal load increased, the frequency of the occurrence of disturbances would decrease. Using the strip chart records, the number of disturbances/unit time were counted as a function of the normal load for all four values of stiffness of the pin arm. It was observed that the transition from a steady state friction process to an unstable one, characterized by the first appearance of self-disturbances, occurred around a normal load of 18–27 N (4–6 lb) for all the stiffnesses investigated. The number of disturbances/unit time is apparently stochastic in its nature.

A SEM photo of the pin surface is shown in Fig. 3(c) for operation in the region of intermittent self-disturbances. In this region of the friction process, the surface, in spite of being smooth and covered with oxide film, shows deep pits and adjoining scratches. The wear process now is no longer only mild or oxidative wear. As seen from Fig. 4, the wear rate sharply increases at the same critical loads (18–27 N) that caused transition from steady to unsteady friction process. It is also clear that the wear rate in this region is much higher than that in steady-state friction process.

(c) **Region of High Frequency Self-Excited Oscillations.** As the normal load is increased still further, it reaches another critical value at which high frequency self-excited vibrations occur and are maintained. It is found that this value of the critical load depends on the system rigidity. This dependence is shown in Fig. 7 where the critical load, at which high frequency self-excited oscillations occur and are maintained,

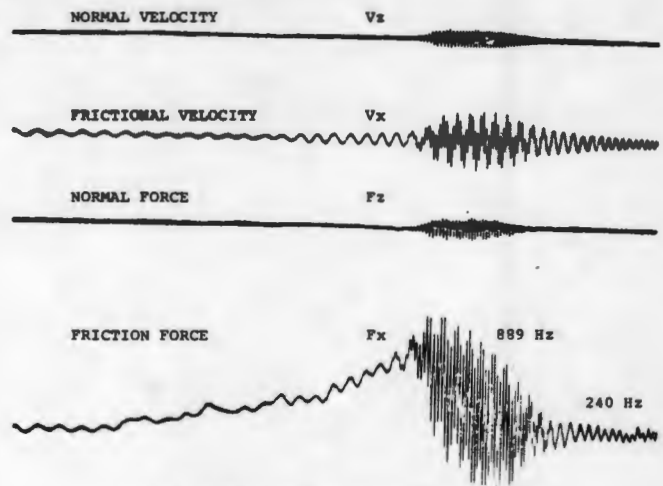


Fig. 6 Friction process at a typical disturbance

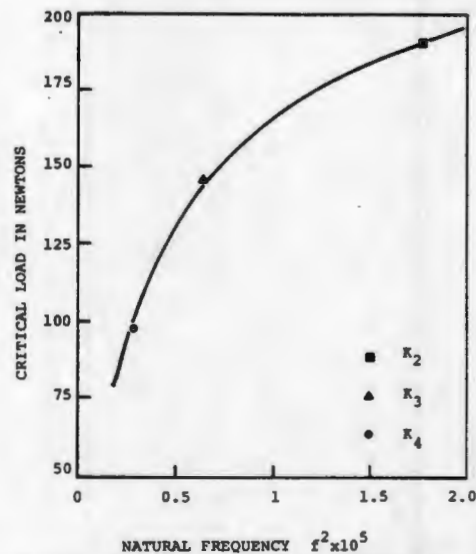


Fig. 7 Critical load causing self-excited vibrations versus the square of the natural frequency

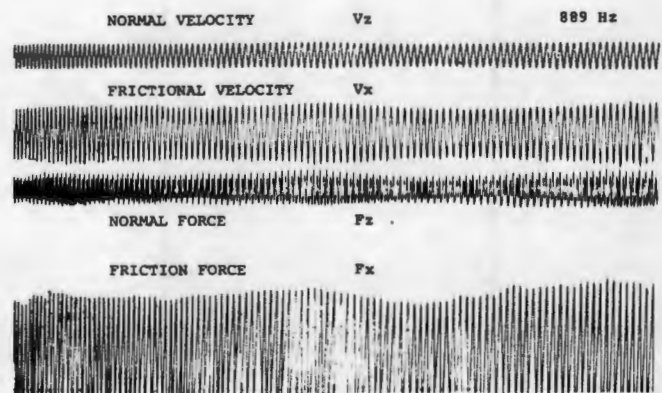


Fig. 8 Self-excited vibrations for stiffness K_3

is plotted versus the square of the natural frequency of the pin not in contact with the disk.

Figure 8 shows the oscillations in the two force components and in the two velocity components in this region for stiffness K_3 . The value of the frequency in this figure is 889 Hz which is seen to be the same as the higher frequency of Fig. 6 during a self-disturbance. The value of this high frequency depends

on the system rigidity and for stiffness K_2 , it is 1045 Hz. These oscillations exhibit a coupling between the frictional and normal degrees of freedom. In this region of high frequency self-excited vibrations, it was noted that a few self-disturbances did also occur.

Figure 3(d) shows a SEM photo of the pin surface taken after running in the region of high frequency self-excited vibrations. Some parts of the surface are smooth with shallow pits without adjoining scratches, whereas other parts exhibit deep pits with adjoining scratches. It has been mentioned earlier that a self-disturbance causes a deep pit with adjoining scratches. Hence, it appears that in the region of self-excited vibrations, the shallow scratches formed earlier are smoothed while the deeper pits still remain as shallow pits on a smooth background. The deep pits with adjoining scratches may have been the result of disturbances that occurred just before the picture was taken where sufficient time was not allowed for the surface to smoothen under self-excited vibrations.

Discussion

From the analysis of the experimental data, an attempt is now made to develop a physical model of the friction processes of boundary lubrication with water. Steady-state friction depends upon the ability of the lubricant and oxide films to separate metallic surfaces from direct contact. This ability is characterized by the kinetics of formation and breakdown of lubricant film between the contacting surfaces. Each of these kinetics is a function of the sliding speed and normal load. With increase in normal load, the dynamic equilibrium of the formation and breakdown of the film is shifted toward an increasing rate of breakdown. Therefore the probability of metallic surfaces coming in direct contact with each other increases with the normal load.

At a certain value of the critical normal load (in these experiments, 18–27 N), direct contact between metallic surfaces becomes inevitable and, finally, direct contact does occur at certain spots. At this stage, transition takes place from steady-state to unsteady-state friction process. Apparently, this transition is independent, or at most weakly dependent, on the system rigidity. Observation of the SEM photos indicate that it is very probable that the deep pits are caused by the formation of metallic junctions, and the scratches are caused by their subsequent shearing. It has been observed earlier that the frequency of occurrence of disturbances was high soon after a change in the normal load and that it would decrease as the elapsed time from a change in the normal load increased. It is understandable that the probability for the formation of junctions would be high after a change in the normal load and would decrease with an increase in the elapsed time.

Using this hypothesis that a self-disturbance is caused by the formation of a metallic junction between the surfaces, the sudden rise in the friction force as seen in Fig. 6 can be attributed to this junction formation. The junction is soon sheared off and the friction force drops back to its nominal value.

The frequency of the low frequency oscillations that appear as soon as the friction force begins its rise in Fig. 6 is seen to be close to the natural frequency of the pin and arm system with the pin not in contact with the disk. It appears that these low frequency oscillations are excited by the unsteadiness of the friction force. When the friction force increases to its high value in Fig. 6, it is now in the range where high frequency self-excited oscillations exist. Hence these high frequency oscillations soon appear. As the friction force decreases back to its nominal value, the high frequency oscillations cannot be maintained and immediately decay to zero. As the system is

very lightly damped, the low frequency oscillations persist for a much longer time as they decay.

In the region of self-excited, high frequency oscillations, there is a coupling between the degrees of freedom in the normal and frictional directions as seen in Figs. 6 and 8, where the two force components and the two velocity components oscillate at the same frequency of 889 Hz. The analysis of these vibrations is currently under way and is not an aim of this paper. Here the conjecture is that the high frequency oscillations are caused by the coupling between the normal and frictional degrees of freedom and the difference in the phase angles of the oscillations. The importance of the coupling between different degrees of freedom has been recognized by Earles and Lee [12] in their linear analysis of the generation of squeal-noise by dry friction.

Some energy is drawn from the steady-state process and is supplied to the vibratory motion. The energy supplied is balanced by the energy dissipated per cycle by damping. This energy transforms mostly into heat, thereby shifting the dynamic equilibrium of formation and breakdown kinetics to an increased rate of formation of lubricant film (in the present case, most probably the formation of oxides). This, then, would explain the near absence of self-disturbances when the operation is in the region of high frequency self-excited vibrations.

The increase of wear rate with an increase in rigidity can be explained as follows: Because of mechanical interactions between contacting surfaces, an increase in rigidity in the normal direction causes an increase in shear force; this, in turn, is responsible for higher wear rate.

Conclusions

From the results of this investigation, which are useful for the design of various equipment such as machinery with moving parts, brakes, bearings, etc., the following conclusions can be drawn.

1 The damage of the frictional surface, indicating transition from mild to severe wear, is caused by breakdown of the lubricant film and by formation and shearing of the adhesive junctions.

2 The breakdown of the lubricant film was observed to occur at some critical normal load independent of the system rigidity. The formation and shearing of junctions cause decaying type of system vibrations.

3 At a certain critical load, continuous self-excited vibrations occur, along with formation and shearing of the junctions. This critical load is a function of the system rigidity and is independent of the breakdown of the lubricant film. In other words, continuous self-excited vibrations can appear before or after formation of the adhesive junctions.

4 The transition in the friction process from the region of steady-state friction to the unstable region of intermittent disturbances causes a transition in the wear process from mild to severe wear.

5 The mild wear rate increases with an increase in the normal load and also with an increase in the system rigidity.

Acknowledgments

This work is based on a U.S. Department of Energy contract on "Study of the Interactions Between Friction, Wear and System Rigidity." We would like to thank Dr. Oscar P. Manley of the Division of Engineering, Mathematical and Geosciences for his support of this project. Thanks are also due to Mr. Eugene Johnson at Illinois Institute of Technology for his assistance on various aspects of this study.

References

- 1 Rabinowicz, E., "A Study of the Stick-Slip Process," *Proceedings of the Symposium on Friction and Wear*, Detroit, 1957, pp. 149-161.
- 2 Ko, P. L., and Brockley, C. A., "The Measurement of Friction and Friction-Induced Vibration," *ASME JOURNAL OF LUBRICATION TECHNOLOGY*, Oct. 1970, pp. 543-549.
- 3 Brockley, C. A., Cameron, R., and Potter, A. F., "Friction-Induced Vibration," *ASME JOURNAL OF LUBRICATION TECHNOLOGY*, Apr. 1967, pp. 101-108.
- 4 Brockley, C. A., and Davis, H. R., "The Time-Dependence of Static Friction," *ASME JOURNAL OF LUBRICATION TECHNOLOGY*, Jan. 1968, pp. 35-41.
- 5 Brockley, C. A., and Ko, P. L., "Quasi-Harmonic Friction-Induced Vibration," *ASME JOURNAL OF LUBRICATION TECHNOLOGY*, Oct. 1970, pp. 550-556.
- 6 Yokoi, M., and Nakai, M., "A Fundamental Study on Frictional Noise," *Bulletin of the J.S.M.E.*, Vol. 22, No. 173, 1979, pp. 1665-1671.
- 7 Bhushan, B., "Stick-Slip Induced Noise Generation in Water-Lubricated Compliant Rubber Bearings," *ASME JOURNAL OF LUBRICATION TECHNOLOGY*, Vol. 102, Apr. 1980, pp. 201-212.
- 8 Krauter, A. I., "Generation of Squeal/Chatter in Water-Lubricated Elastomeric Bearings," *ASME JOURNAL OF LUBRICATION TECHNOLOGY*, (in press).
- 9 Welsh, N. C., "Frictional Heating and Its Influence on the Wear of Steel," *J. of Appl. Phys.*, Vol. 28, No. 9, Sept. 1957, pp. 960-968.
- 10 Archard, J. F., "Temperature of Rubbing Surfaces," *Wear*, Vol. 2, 1959, pp. 438-454.
- 11 Lancaster, J. K., "The Influence of the Conditions of Sliding on the Wear of Electrographitic Brushes," *Brit. J. Appl. Phys.*, Vol. 13, No. 9, Sept. 1962, pp. 468-477.
- 12 Earles, S. W. E., and Lee, C. K., "Instabilities Arising from the Frictional Interactions of a Pin-Disk System Resulting in Noise Generation," *ASME Journal of Eng. for Industry*, Vol. 98, 1976, pp. 81-86.

APPENDIX 2



The Society shall not be responsible for statements or opinions advanced in papers or in discussion at meetings of the Society or of its Divisions or Sections, or printed in its publications. Discussion is printed only if the paper is published in an ASME Journal. Released for general publication upon presentation. Full credit should be given to ASME, the Technical Division, and the author(s). Papers are available from ASME for nine months after the meeting.
Printed in USA.

Interactions Among Friction, Wear and System Stiffness—Part 1: Effect of Normal Load and System Stiffness

V. Aronov
A. F. D'Souza
S. Kalpakjian
I. Shareef

Department of Mechanical Engineering,
Illinois Institute of Technology,
Chicago, Ill. 60616

Dry frictional contact between two metallic surfaces, one cast iron and the other steel, is analyzed. The experiments were conducted using a pin-on-disk setup instrumented with force and acceleration transducers. The interactions between friction, wear, and vibrations and their dependence on normal load and system stiffness are investigated. The results indicate that stiffness has a significant effect on the normal load at which transition takes place from mild to severe friction and wear. The variation of surface roughness with normal load for different stiffnesses is also examined. The different regimes of friction are observed, as the normal load is increased. They are characterized as steady state friction region, nonlinear friction region, region of transient friction with disturbances and region of self-excited vibrations. It is shown that the transition from the steady-state friction can be characterized by a sudden increase in the coefficient of friction and amplitude of slider oscillations.

Introduction

The subject of friction and wear between sliding surfaces has been studied extensively for many years in terms of their controlling factors and parameters such as materials, surface conditions, loads, speed, temperature, environment, and lubricants. Various theories have been proposed concerning the mechanisms of friction and wear, and numerous attempts have been made to establish quantitative relationships between the many parameters involved.

However, little attention has been paid in the past to the effect of friction and wear due to system stiffness, i.e., dynamic characteristics of the equipment, machinery, or test facility. Different types of vibrations induced by friction have been studied separately by several investigators including Soom and Kim [1], Ko and Brockley [2], and Bhushan [3]. Rice [4] has investigated sliding and impact wear and has observed that different wear behaviors can result from variation in the specimen length which, in his setup, corresponds to variation in stiffness. It is recognized that several different mechanisms can be operative as a result of changes in parameters. But the effect of system stiffness has not received much attention and the conditions under which transition takes place from one type of behavior to another are difficult to establish.

In an earlier study [5], the authors have reported the effect of normal load and system stiffness on friction and wear and water lubrication. They observed that, in the case of boundary lubrication with water, the transition from mild to severe friction and wear depends on the normal load but is nearly independent of system stiffness. The mild wear rate, however, increases with stiffness and friction-induced vibrations are stiffness dependent.

This paper describes the results of an experimental investigation of the effects of system stiffness on friction, wear and vibrations and their variations with normal load. Experiments were conducted using a pin-on-disk setup with a steel pin sliding on a cast iron disk without lubrication. The values of the normal load for transition from mild to severe friction and wear are presented for different stiffnesses, and the surface roughness is examined. Different friction regimes in dry sliding conditions are discussed.

Experimental Setup and Procedure

Apparatus. Measurements were made with a pin-on-disk type sliding friction apparatus instrumented with piezoelectric force and acceleration transducers. A general view of the test apparatus is shown in Fig. 1, and an extensive description of the associated instrumentation is given elsewhere [5]. Briefly stated, the apparatus consists of a rotating disk, 200 mm in diameter, driven by a 1 hp a-c motor through a variable-speed drive which gives a speed range from 0 to 700 rpm.

The pin, which represents a stationary mating surface is 5

Contributed by the Lubrication Division of THE AMERICAN SOCIETY OF MECHANICAL ENGINEERS for presentation at the ASME/ASLE Joint Lubrication Conference, Hartford, Conn., October 18-20, 1983. Manuscript received by the Lubrication Division, March 27, 1983. Paper No. 83-Lub-34.
Copies will be available until July 1984.

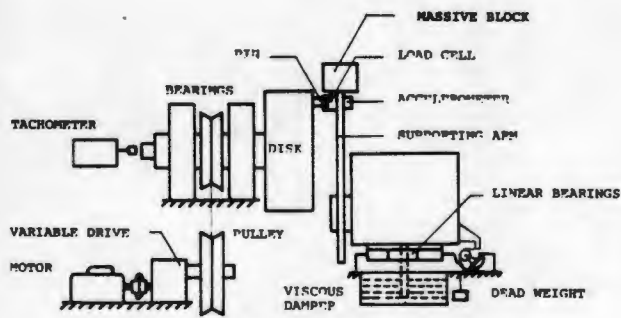


Fig. 1 Schematic of test apparatus

mm in diameter. An expansion bolt serves to grip the pin at one end and an accelerometer at the other, while the force transducer is sandwiched with preload of 25 kN between bolt head and supporting arm. The supporting arm, whose length can be varied by changing the position of the clamp, is used as a spring with variable stiffness. Strain gages fixed on the supporting arm were used to record continuously the friction force f_x , on a strip chart recorder. The variations in the friction force, F_x , and normal force, F_z , were sensed by piezoelectric transducers and were recorded on a Visicorder.

Materials. A special quality steel 0.5 percent C, 0.85 percent Mn, 0.04 percent P and 0.05 percent S, quenched and hardened to 48 HRC was used as pin material. The material of the disk was cast iron.

Test Procedure. The pin and disk were lapped in situ with 600 grit lapping compound to a smooth finish (0.5 μm CLA) under a normal load of 8 N (1.8 lb). Special care was taken to ensure clean surfaces by cleaning with methanol and acetone. The pin was brought in contact with the revolving disk at 8 N normal load and, in this state, the pin was allowed to run in for a distance of approximately 12-15 Km to ensure that a stable steady state friction process has been achieved. After this, the normal load was increased in steps of 4.5 N (1 lb) up to a load of 26 N and then the load was increased in steps of 9 N (2 lb). The time between any two consecutive loadings was maintained at around thirty minutes.

At each normal load, the analog wave form of the dynamic components, F_x and F_z in frictional and normal forces and the corresponding velocities V_x and V_z were recorded on a Visicorder oscillograph. A spectral analyzer was used to analyze the analog signals to obtain the spectra SF_x , SF_z , SV_x , and SV_z of forces F_x , F_z and velocities V_x , V_z , respectively.

Three sets of experiments were conducted for supporting arm lengths of 5.1 cm (2 in.), 8.9 cm (3.5 in.), and 12.7 cm (5 in.) corresponding to stiffnesses K_1 , K_2 , and K_3 , respectively, in decreasing order. All sets of experiments have been repeated at least two times. However, in the results presented in the next section, only the most representative data is shown in order to indicate the trend. The modal frequencies of the system for these stiffnesses are given in the companion paper [6]. In all experiments reported here, the sliding speed was maintained constant at 46 cm/s. For each arm length, the rate and magnitude of normal loading and the recording of various parameters at each load were performed in the same manner as stated in the preceding. All experiments were

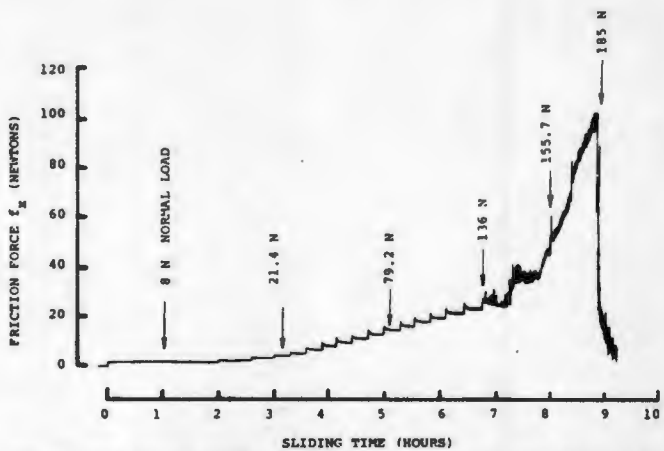


Fig. 2 Strip chart record of friction force variation with increase in normal load and time for 5.1 cm arm length

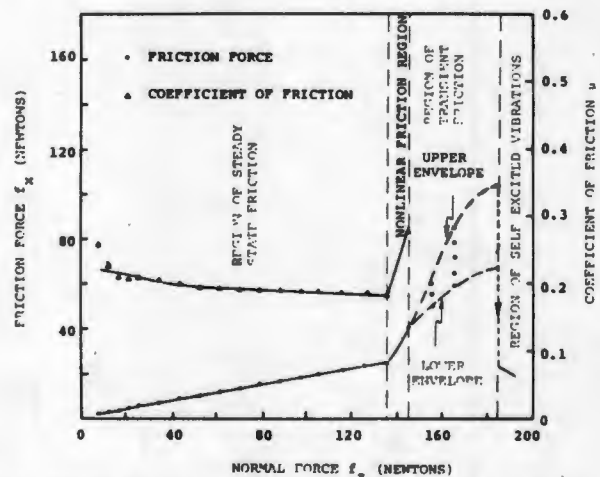


Fig. 3 Friction force and coefficient of friction versus normal force for sliding speed of 46 cm/s and arm length 5.1 cm (2 in.)

performed in ambient environment where the temperature ranged from 20 to 23° C (68 to 73° F) and relative humidity of 50 to 60 percent.

Experimental Results

A typical strip-chart record of the strain gage measurement of the steady state friction force f_x is shown in Fig. 2 for stiffness K_1 , corresponding to an arm length of 5.1 cm. Four different regimes of friction are observed depending on the normal load. These regimes are shown in Fig. 3 and are classified as steady state friction region, nonlinear friction region, region of transient friction with disturbances, and self-excited vibration region. The detailed behavior in these four regions is discussed in the following.

Steady State Friction Region. As the normal load is increased in steps, up to 136 N, the friction force increases linearly with the normal load, as seen in Fig. 3. For small

Nomenclature

F_x = oscillatory component of friction force	SF_x = spectrum of F_x	
f_x = friction force	SF_z = spectrum of F_z	
F_z = oscillatory component of normal force	SV_x = spectrum of velocity in frictional direction	V_x = pin velocity in frictional direction
f_z = normal force	SV_z = spectrum of velocity in normal direction	V_z = pin velocity in normal direction

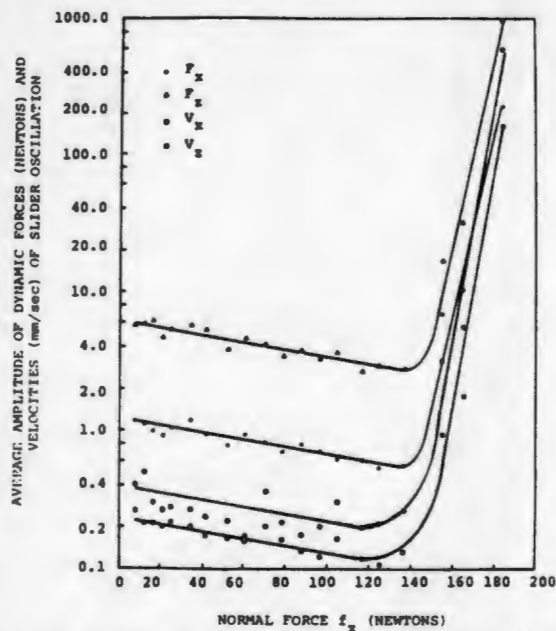


Fig. 4 Average amplitude of dynamic forces and velocities in frictional and normal directions versus normal force at sliding speed of 48 cm/s and for arm length 5.1 cm (2 in.)

normal loads, there is an initial decrease in the coefficient of friction, but it stabilizes to a nearly constant value in this region. During the time between loadings, the mean value of the friction force remains constant. Small oscillations in the force and slider velocities were observed in this region. Most likely, they were induced by random surface irregularities. The mean values of the amplitudes of the force oscillations F_x and F_z and also those of the velocities V_x and V_z decrease with increasing normal load in this region, as shown in Fig. 4. Wear measurements, as reported in the companion paper [7], indicate that low rates of wear occur in this region.

Nonlinear Friction Region. This region is shown in Fig. 3 for normal loads ranging from 136 to 146 N. In this region, the friction force increases nonlinearly with the normal load. The coefficient of friction is no longer constant and independent of the normal load but increases with it. During the time between loadings, the mean value of the friction force remains constant as in the first region. But the mean values of the amplitudes of the force oscillations and velocities increase with increasing normal load, as shown in Fig. 4. Wear measured in this region is found to be several times larger than that measured in steady state friction region.

Region of Transient Friction With Disturbances. When the normal load lies in the range from 146 to 185 N in Fig. 3, the mean value of the friction force does not remain constant between the loading steps as seen in Fig. 2. It was observed that the mean value of the friction force increases with time at a constant normal load. There are also disturbances and the mean value of the friction force intermittently increases and decreases without any external excitation. When the mean friction force reached a sufficiently high value, a temporary burst of self-excited vibrations would occur and the friction force would instantly fall to a lower value.

Region of Self-Excited Vibrations. When the normal load is increased beyond 185 N, the mean friction force drops to a very low value, as seen in Fig. 2, but it is accompanied by high-amplitude periodic self-excited oscillations in forces and slider velocities. All four oscillations have the same dominant (highest amplitude) frequency which corresponds to the torsional frequency of the system about the longitudinal axis of the slider arm. The importance of these torsional vibrations

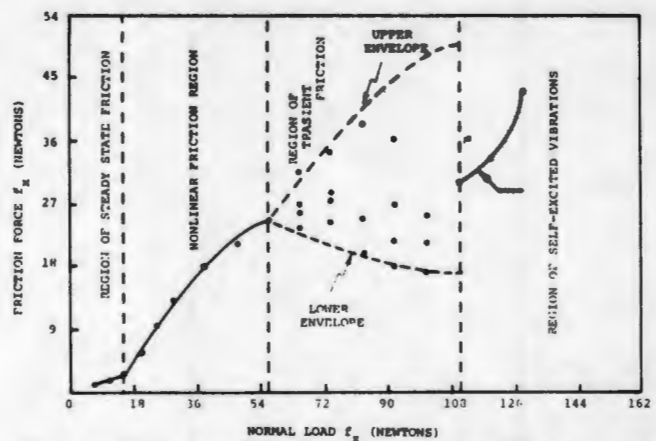


Fig. 5 Friction force versus normal force for sliding speed of 48 cm/s and arm length of 1.27 cm (5 in.)

has also been observed earlier in a similar pin-on-disk experimental investigation [8]. As observed from the high amount of wear debris produced in this region, wear is found to be several orders of magnitude higher than that in the nonlinear friction region.

The variation of the mean friction force with normal load is shown in Fig. 5 for the least stiff spring (K_3) corresponding to the arm length of 12.7 cm. The four different regimes of operation are again observed but the effect of system stiffness becomes apparent. The region of steady state friction, where the friction force increases linearly with the normal load and the coefficient of friction is constant, has shrunk in Fig. 5 to a normal load of about 15 N. The region of nonlinear friction, where the coefficient of friction increases with the normal load, extends from 15 to 56 N normal load.

When the load lies in the range of 56 to 110 N in Fig. 5, a region of transient friction was observed. In this region, the mean value of the friction force increases with time for a constant value of the normal load. When it reaches a sufficiently high value, a burst of self-excited vibrations occurs. The friction force instantly falls to a lower value, the self-excited vibrations disappear and the process is repeated. The upper and lower envelopes of the mean value of the friction force are shown in Fig. 5. The mean value of the friction force lies within this envelope at a given time.

The region of self-excited vibrations is observed when the normal load is beyond 110 N. However, it is seen from Fig. 5 that the mean value of the friction force, about which oscillations occur, is now quite high as compared to the low value observed for the stiffest spring K_1 and the intermediate spring K_2 .

The normal load at which transition occurs from steady state friction to nonlinear friction plays a very important role in wear. Our wear measurements show that it is the critical normal load which is responsible for transition that takes place from mild to severe wear. The critical normal load is shown in Fig. 6 for the three stiffnesses. It is seen that the critical load is proportional to the system stiffness.

The surface of the slider pin was examined with a Talysurf profilometer for the surface profiles and roughnesses in the region of steady state friction. The variation of the pin surface roughness with the normal load for the same sliding distance is shown in Fig. 7 for the three stiffnesses in the region of steady state friction. Several observations can be made from this figure.

The roughness along the direction of sliding is much smaller than that across the sliding direction for all normal loads and stiffnesses. The roughness across the sliding direction is largest for the stiffest spring K_1 and decreases with the

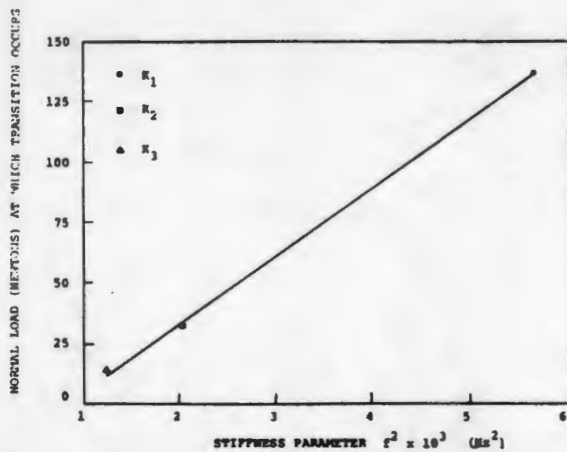


Fig. 6 Plot of the critical load at which transition in friction process occurs versus the stiffness parameter for three stiffnesses K_1 , K_2 , and K_3

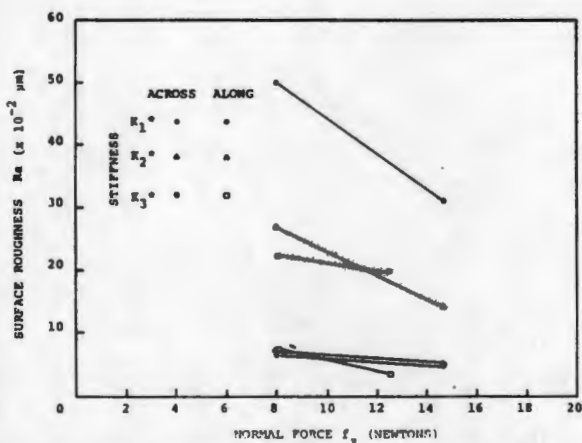


Fig. 7 Variation of surface roughness across and along the lay with normal force for three stiffnesses

stiffness. Also, the roughness decreases with normal load. The roughness along the direction of sliding is not very sensitive to stiffness and decreases slightly as the normal load is increased. The variation of roughness as a function of the square of the natural frequency in the frictional direction corresponding to the stiffness is shown in Fig. 8 for a normal load of 8 N. It is seen that the roughness across the sliding direction is proportional to the square of the natural frequency but the roughness along the direction of sliding is insensitive to stiffness. Also, the surface roughness across the sliding direction decreases with sliding distance, as shown in Fig. 9, while the roughness along the direction of sliding remains almost constant.

Discussion

It is clear from the results that for sliding friction without lubrication, the mean value of the friction force is proportional to the normal load only in the region of steady state friction. In the region of nonlinear friction, the coefficient of friction depends on the normal load even though the mean value of friction force remains constant with time for a constant normal load.

It has been observed that in the region of steady-state friction, the amplitudes of oscillations of forces and velocities decrease as the normal load is increased (Fig. 4). At the same time the surface roughness decreases with normal load in that region as shown in Fig. 7. The oscillations and vibrations in that region appear to be induced by surface roughness as analyzed by Soom and Kim [1]. Also, we have observed that

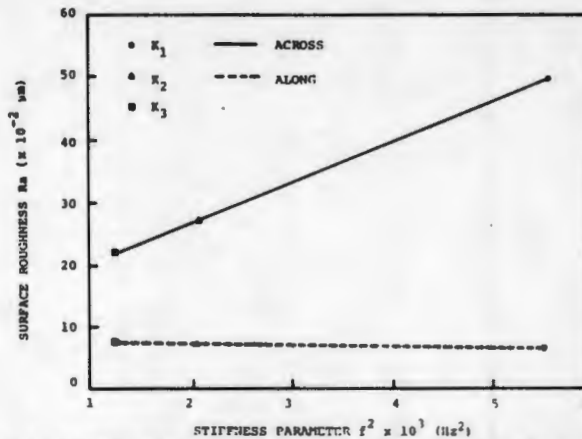


Fig. 8 Variation of surface roughness across and along the lay with stiffness parameter for three stiffnesses K_1 , K_2 , and K_3

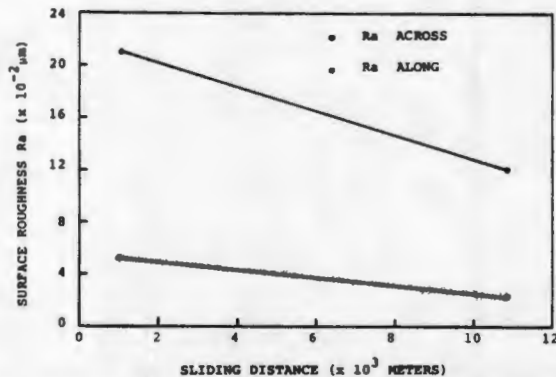


Fig. 9 Variation of surface roughness with sliding distance for stiffness K_1 at normal load of 22 Newtons

in this region the surface roughness decreases with sliding distance, as shown in Fig. 9.

After the transition from the steady state friction region, the amplitudes of oscillation increase with normal load (Fig. 4) and also with sliding distance. This is an indication that after the transition, the surface gradually gets damaged and the roughness increases. This is confirmed by the observation that the transition from steady state friction also corresponds to the transition from mild to severe wear.

In the region of self-excited vibrations, the mean value of the friction force is high for stiffness K_3 , as seen from Fig. 5, whereas it is quite low for stiffness K_1 in Fig. 2. The self-excited vibrations are analyzed for stiffness K_3 in the companion paper [6] and the measurements indicate that the slider did not lose contact with the disk during the oscillations. It is quite likely that for stiffness K_1 the contact between the slider and the disk was lost during a part of the cycle.

Conclusions

The following conclusions can be drawn from this study.

1. Four regimes of friction are encountered in sliding of steel on a cast iron surface without lubrication. The steady state friction regime is characterized by a coefficient of friction that is independent of the normal load, small rate of wear (mild wear), absence of surface damage, smoothing of the surface and small amplitude of slider oscillations.

The region of nonlinear friction is characterized by coefficient of friction that increases with normal load, large rate of wear (severe wear), increase in the amplitude of slider oscillations with normal load and increase in surface roughness.

In the region of transient friction, the friction force varies

with time for a constant normal load so that a coefficient of friction cannot be defined and there are self-disturbances that cause sharp increase and decrease of the friction force. This is a region of severe wear and surface damage.

The self-excited vibration region is characterized by periodic oscillations of the slider and a wear rate several orders of magnitude higher than that observed in any other region.

2. The transition from mild to severe wear corresponds to the transition in steady state friction and can be characterized by a sharp increase in the coefficient of friction and amplitudes of slider oscillations.

3. The range of the region of steady state friction can be increased by increasing the system stiffness for unlubricated contact.

4. In the region of steady state friction, the amplitudes of the contact oscillations depend on the surface roughness which is a decreasing function of the normal load and an increasing function of the stiffness.

Acknowledgments

This study was sponsored by the U.S. Department of Energy, Contract No. DE-AC02-82ER12071 on "Interactions Between Friction-Induced Vibration and Wear." We would like to thank Dr. Oscar P. Manley of the Division of Engineering, Mathematical and Geosciences, U.S. Department

of Energy, for his support of this project. Thanks are also due to Mr. F. Dream, former graduate student, for his assistance. This paper is based partly on the Ph.D. dissertation of I. Shareef.

References

- 1 Soom, A., and Kim, C., "Roughness-Induced Dynamic Loading at Dry and Boundary-Lubricated Sliding Contacts," *ASME JOURNAL OF LUBRICATION TECHNOLOGY* (in press).
- 2 Ko, P. L., and Brockley, C. A., "The Measurement of Friction and Friction-Induced Vibration," *ASME JOURNAL OF LUBRICATION TECHNOLOGY*, Oct. 1970, pp. 543-549.
- 3 Bhushan, B., "Stick-Slip Induced Noise Generation in Water-Lubrication Compliant Rubber Bearings," *ASME JOURNAL OF LUBRICATION TECHNOLOGY*, Apr. 1980, pp. 201-212.
- 4 Rice, S. L., Hans, N., and Steven, F. W., "The Role of Specimen Stiffness in Sliding and Impact Wear," *Wear*, Vol. 77, 1982, pp. 13-28.
- 5 Aronov, V., D'Souza, A. F., Kalpakjian, S., and Shareef, I., "Experimental Investigation of the Effect of System Rigidity on Wear and Friction-Induced Vibrations," *ASME JOURNAL OF LUBRICATION TECHNOLOGY*, Apr. 1983, pp. 206-211.
- 6 Aronov, V., D'Souza, A. F., Kalpakjian, S., and Shareef, I., "Interactions Among Friction, Wear and System Stiffness—Part 2: Vibrations Induced by Dry Friction," *ASME JOURNAL OF LUBRICATION TECHNOLOGY* (to appear).
- 7 Aronov, V., D'Souza, A. F., Kalpakjian, S., and Shareef, I., "Interactions Among Friction, Wear and System Stiffness—Part 3: Wear Model," *ASME JOURNAL OF LUBRICATION TECHNOLOGY* (to appear).
- 8 Earles, S. W. E., and Lee, C. K., "Instabilities Arising From the Frictional Interaction of a Pin-Disk System Resulting in Noise Generation," *ASME Journal of Engineering for Industry*, Feb. 1976, pp. 81-86.

APPENDIX 3



The Society shall not be responsible for statements or opinions advanced in papers or in discussion at meetings of the Society or of its Divisions or Sections, or printed in its publications. Discussion is printed only if the paper is published in an ASME Journal. Released for general publication upon presentation. Full credit should be given to ASME, the Technical Division, and the author(s). Papers are available from ASME for nine months after the meeting.

Printed in U.S.A.

Interactions Among Friction, Wear, and System Stiffness—Part 2: Vibrations Induced by Dry Friction

V. Aronov

A. F. D'Souza

S. Kalpakjian

I. Shareef

Department of Mechanical Engineering,
Illinois Institute of Technology,
Chicago, Ill. 60616

Different types of vibrations induced by dry friction are investigated by means of a model apparatus described in Part 1. The structural model is obtained from the measurement of the modal frequencies and damping ratios of three degrees of freedom. The oscillations in the normal and frictional forces, as well as the slider vibrations, have been measured and analyzed. As the normal load is increased, four different regions of vibrations are observed corresponding to the four friction regimes discussed in a companion paper. Small oscillations are encountered at low values of the normal load and they are possibly caused by random surface irregularities. The vibration characteristics are changed when transition occurs from steady state friction. When the normal load is further increased, self-excited periodic vibrations are produced. The spectra of the oscillations are related to the modal frequencies. Self-excited vibrations are analyzed on the basis of the experimental data.

Introduction

A wide variety of systems have components such as clutches, brakes, and commutator brushes where one surface slides over another at a relative velocity under the action of dry friction. In such systems, different types of friction induced vibrations have been frequently observed under certain conditions. These vibrations are undesirable due to their detrimental effects. The squeal and chatter that they produce can cause excessive wear of components, severely damage the surfaces, lead to fatigue failure and may reach objectionable noise levels.

The subject of friction induced vibrations has been studied by several investigators in the past. Different types of vibrations induced by friction have been reported in the literature depending on the normal load, sliding speed, and the nature of the surfaces in contact. It is apparent that there exist several distinct mechanisms that can excite different types of oscillations. These vibrations may be generally classified in the following three classes: Stick-slip, vibrations induced by random surface irregularities, and quasi-harmonic self-excited oscillations.

Stick-Slip. These vibrations, which occur when the sliding speed is sufficiently low, are periodic and as observed by Ko and Brockley [1], they have almost a saw-tooth waveform because the relative velocity between the surfaces is zero

during the stick part of the cycle. The mechanism that causes stick-slip is attributed to the fact that the static and kinematic coefficients of friction are different and static friction requires some time to build up to its steady-state value after the surfaces in contact come to rest with respect to each other [2]. As the sliding speed is increased, there is a critical value of the speed above which stick-slip type of vibrations disappear [2].

Vibrations Induced by Random Surface Irregularities. At sufficiently low values of the normal load, small oscillations have been observed by several investigators including Soom and Kim [3, 4] and also have been reported by the present authors [5]. They are possibly induced by randomly distributed surface irregularities as analyzed by Soom and Kim [4]. The power spectral density of the oscillations exhibits a peak for each of the structural modes. The integral of the power spectral density over the frequency range yields the mean square value.

Quasi-Harmonic Oscillations. These oscillations, which occur when the sliding speed and normal load are sufficiently high, are periodic and their waveform is nearly sinusoidal. For this reason, they have been named quasi-harmonic vibrations by Brockley and Ko [6] in order to distinguish them from stick-slip vibrations with a saw-tooth waveform. The mechanism that causes quasi-harmonic oscillations has been attributed by Brockley and Ko [6], Krauter [7] and several other investigators to the fact that in certain regions, the steady-state friction versus sliding speed curve has a negative slope which can supply energy to the oscillations.

Contributed by the Lubrication Division of THE AMERICAN SOCIETY OF MECHANICAL ENGINEERS for presentation at the ASME/ASLE Joint Lubrication Conference, Hartford, Conn., October 18-20, 1983. Manuscript received by the Lubrication Division, March 27, 1983. Paper No. 83-Lub-35.

Copies will be available until Aug. 1984.

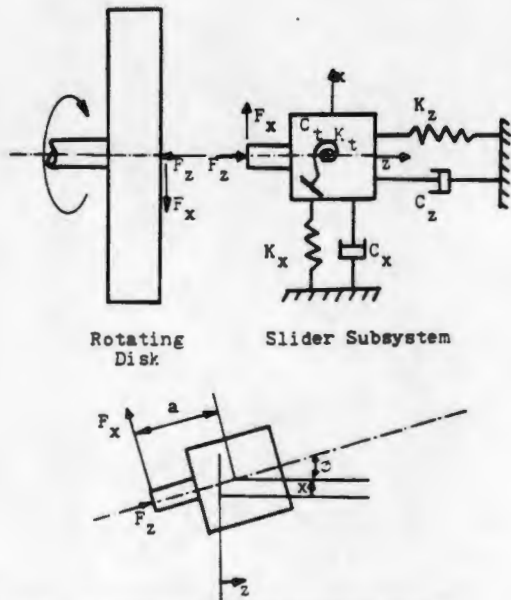


Fig. 1 Mathematical model of the slider system

In their experiments of sliding with dry friction, Yokoi and Nakai [8] have observed quasi-harmonic vibrations which they named squeal. These vibrations occurred not only in the region where the slope of the steady-state friction versus sliding velocity is negative, but also in the region where it is positive. They state that their experimental results are inconsistent with the frictional vibration theory that self-excited vibrations are not generated when the slope of the friction force versus sliding speed is positive. Jarvis and Mills [9] state that in their study, the variation of the coefficient of friction with relative velocity was insufficient to cause the vibrations induced by dry friction. It appears that different types of quasi-harmonic oscillations are possible and can be induced by different mechanisms.

The study reported in this paper deals with the investigation of different types of vibrations observed in dry friction experiments. Experiments were conducted with a pin-on-disk type setup instrumented with piezo-electric force and acceleration transducers and strain-gages. The details of the experimental setup and instrumentation are given in a companion paper [11] and are omitted here. The sliding speed was sufficiently high that stick-slip did not occur but vibrations induced by random surface irregularities and quasi-harmonic oscillations were observed as the normal load was varied.

Structural Dynamic Model. The dynamic model of the structure plays an important role in the vibrational response. Based on the experimental results discussed later, a three-degree-of-freedom model is shown in Fig. 1. In this figure, the z -axis is in the normal direction and its positive direction is

away from the disk. The x -axis is the direction of the friction force on the pin and the y -axis is in the vertical direction. The three degrees of freedom correspond to the translation in the normal and frictional directions and torsion about the y -axis. Other degrees of freedom are negligible as the system is very stiff in those directions. Let F_z and F_x denote the oscillating components of the normal and frictional forces, respectively. Their positive directions are as shown in Fig. 1.

The natural frequencies and damping ratios of the three degrees of freedom were determined experimentally for the following two cases: Pin not in contact with the disk and pin in contact with the running disk. The pin was hit impulsively in the normal and frictional directions, respectively. The block was also hit impulsively off-center to determine torsional natural frequency and damping about the vertical axis. The spectra of the impulse responses of the accelerometer in both the normal and frictional directions were analyzed by the Fourier analyzer. The impulse responses were also recorded with a storage oscilloscope.

The damped natural frequencies were obtained from the peaks of the impulse response spectra. The damping ratios were determined for stiffness K_3 , and also the natural frequencies were verified from the display of the experimental impulse responses in the normal, frictional and torsional directions, respectively, in the time domain on a storage oscilloscope. The typical impulse response in the frictional direction without contact between the pin and disk is shown in Fig. 2(a) and with contact between the pin and running disk with a normal load of 20 N (4.5 lb) is shown in Fig. 2(b). It is observed that the modes are very lightly damped. The method of logarithmic decrement was employed to determine the damping ratios. The experimentally obtained natural frequencies are shown in Table 1. The normal load when the pin was in contact with the running disk was 20 N (4.5 lb).

When the slider is in contact with the disk under normal load, the arm with slider becomes very stiff in the normal direction and the natural frequency in the normal direction is very high. However, several natural frequencies of the base could be observed.

Experimental Investigation of Vibrations. Three sets of experiments were conducted as reported in the companion paper [11] for supporting arm lengths of 5.1 cm (2 in.), 8.9 cm (3.5 in.) and 12.7 cm (5 in.) corresponding to stiffnesses K_1 , K_2 , and K_3 , respectively. In all the experiments reported here, the sliding speed between the steel slider and cast iron disk was maintained constant at 46 cm/s. It is stated in reference [11] that four different regions of operation were observed as the normal load was increased. The vibrations induced by dry friction in these regions are discussed in the following.

Small oscillations in the contact forces and slider velocities occur in the region of steady state friction. Typical waveforms in this region as recorded on the Visicorder oscillograph are shown in Fig. 3 for stiffness K_1 and normal load of 16.9

Nomenclature

a = moment arm of the force F_x
 c_1, c_x, c_z = coefficient of damping
 F_x = oscillatory component of friction force
 F_z = oscillatory component of normal force
 I = mass moment of inertia about y -axis
 K_1, K_2, K_3 = stiffness parameter
 k_1, k_x, k_z = spring constant

m = effective mass
 t = time
 V_x = pin velocity in frictional direction
 V_z = pin velocity in normal direction
 W_s, W_d = work done per cycle
 x = oscillatory component of pin displacement in frictional direction

z = oscillatory component of pin displacement in normal direction
 τ_1, τ_1, τ_2 = phase angle
 ξ_1, ξ_x, ξ_z = damping ratio
 ϕ = torsional displacement about y -axis
 ω = frequency
 $\omega_{n1}, \omega_{nx}, \omega_{nz}$ = natural frequency

Table 1 Natural frequencies and damping ratios

Stiffness	Direction	Pin not in contact with disk		Pin in contact with running disk	
		Damped natural frequency Hz	Damping ratio	Damped natural frequency Hz	Damping ratio
K_1	Frictional	69		69	
	Normal	66			
	Torsional	126		125	
K_2	Frictional	45		49	
	Normal	50			
	Torsional	102.5		101	
K_3	Frictional	32.5	0.0069	32.5	0.0038
	Normal	35	0.0089		
	Torsional	85	0.0043	86.25	0.0058

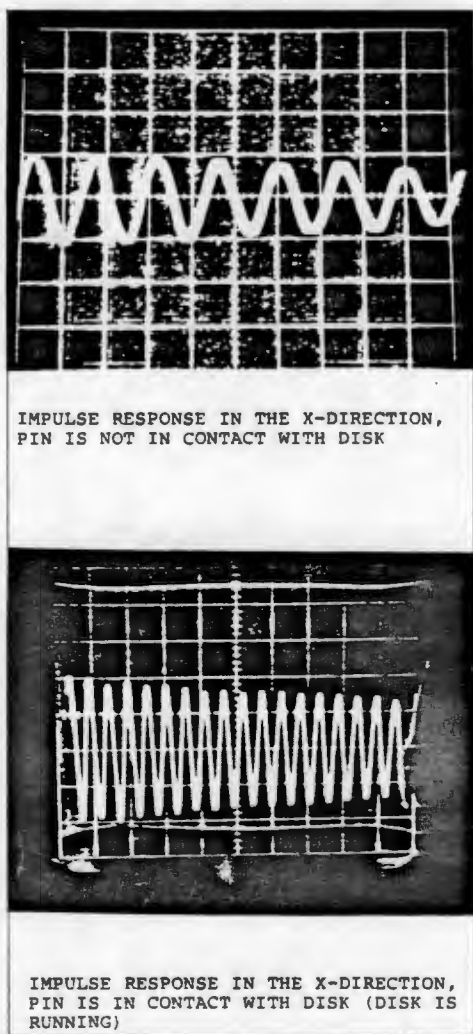


Fig. 2 Typical impulse response in the frictional direction with and without contact between pin and disk

N. The spectra of the oscillations in the normal and frictional forces obtained by the spectral analyzer are also shown in this figure. The power spectral density exhibits a peak for each of the structural modes of the base in the normal direction. The natural frequencies of the pin-arm are not excited. The frequency of 120 Hz is the frequency of vibration of the motor casing.

The amplitude and mean square value of the oscillations decrease in this region as the normal load increases. It appears

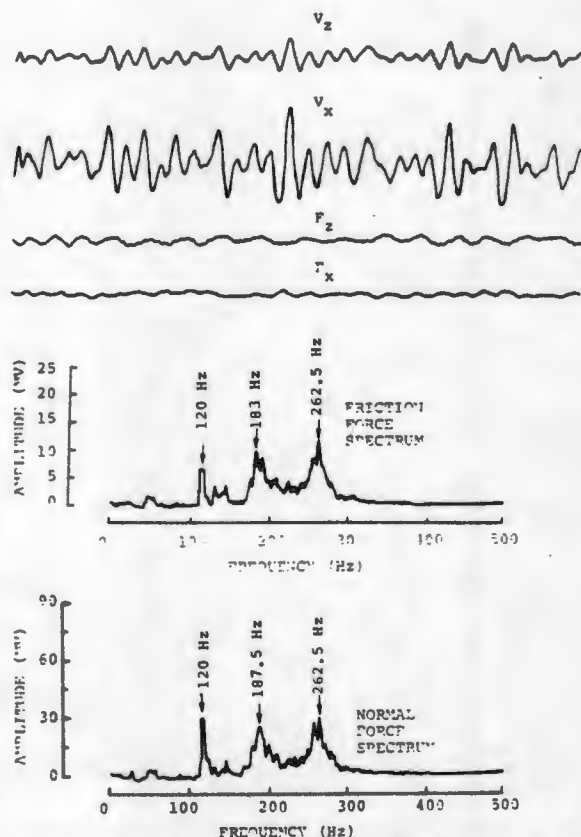


Fig. 3 Typical wave forms and spectra of oscillations in the normal and frictional direction, in the region of steady state friction

that the base frequencies are excited by random surface irregularities. The run-in surfaces have irregularities that are stochastic. It is shown in [11] that in the region of steady state friction, the surface roughness decreases as the normal load is increased. Consequently, the amplitudes of the oscillations also decreased.

The vibration characteristics change when transition occurs in the steady state friction. It is observed in [11] that the surface roughness increases with the normal load after transition and hence, the amplitudes of oscillations also increase with the normal load. Typical wave-forms recorded on the Visicorder oscillograph and the spectra of the oscillations in the normal and frictional forces are shown in Fig. 4 for stiffness K_1 for normal load of 146 N in the region of nonlinear friction. The cause of these oscillations is stochastic in nature. It is interesting to note that the peak frequencies in Fig. 4 are quite different from those shown in Fig. 3. The

dominant frequency of 69 Hz in Fig. 4 corresponds to the modal frequency of the slider arm in the frictional direction and the second peak frequency of 125 Hz is the torsional mode frequency.

In the region of transient friction, the mean value of the friction force, which changes with time for a constant value of normal load, is accompanied by oscillations whose amplitudes increase with the mean value of the friction force. Their

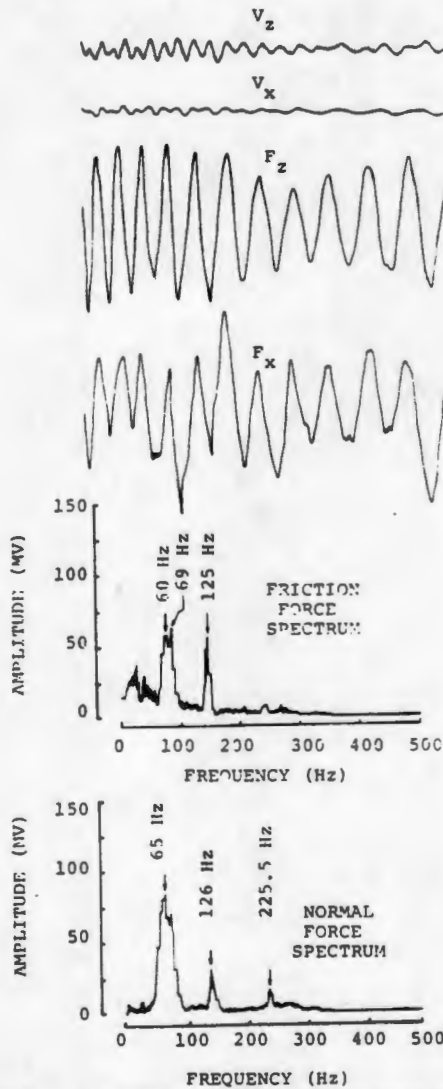


Fig. 4 Wave forms and spectra of forces and velocities in the region of nonlinear friction

frequencies were the same peak frequencies that are shown in Fig. 4. Also, when the mean value of friction force was sufficiently high, short temporary bursts of self-excited oscillations were observed.

The region of self-excited oscillations is reached when the normal load is increased to a sufficiently high value. These oscillations are periodic and have high amplitudes. The wave-forms of the self-excited oscillations are shown in Fig. 5 for stiffness K_3 and normal load of 110.3 N (24.5 lb). The frequency of these self-excited oscillations as observed on the Fourier analyzer is 86.25 Hz which is the torsional mode frequency of the slider-arm system. Hence it can be concluded that the torsional degree of freedom is mainly responsible for the cause of the self-excited oscillations. Earles and Lee [12] have also made similar observations regarding the importance of torsional oscillations in their setup.

The spectra of the slider velocities V_x and V_z and of the oscillatory components F_x and F_z of the forces are shown in Fig. 6. The slider velocity in the frictional direction also has a smaller peak at 32.5 Hz which is the modal frequency of the slider-arm system in the frictional direction. It is observed from Fig. 5 that the wave-forms of the slider velocities are nearly sinusoidal but the wave-form of the forces are distorted by the second harmonic components riding on the fundamental frequency as seen from Fig. 6.

The Visicorder paper was run at a speed such that the peak to peak distance in Fig. 5 is 35 mm. The phase angles among the four oscillations can be determined by measuring the distances between their respective peaks. The four channels of the Visicorder were calibrated so that the forces could be read in Newtons and the velocities in m/s. Using these calibrations, the expressions for the fundamental components of the four

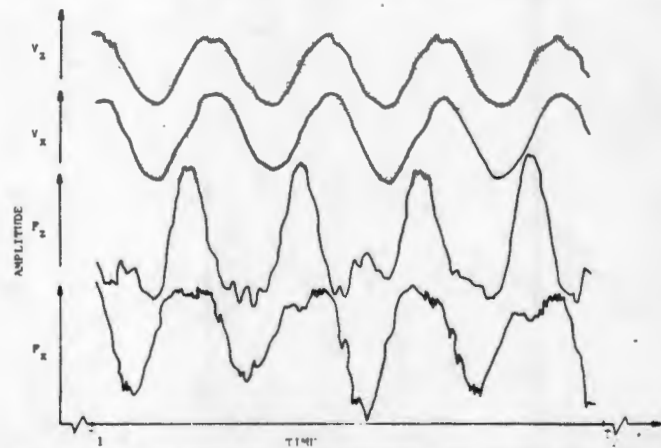


Fig. 5 A typical trace of forces and velocities during self-excited vibration for 110.3 N normal load

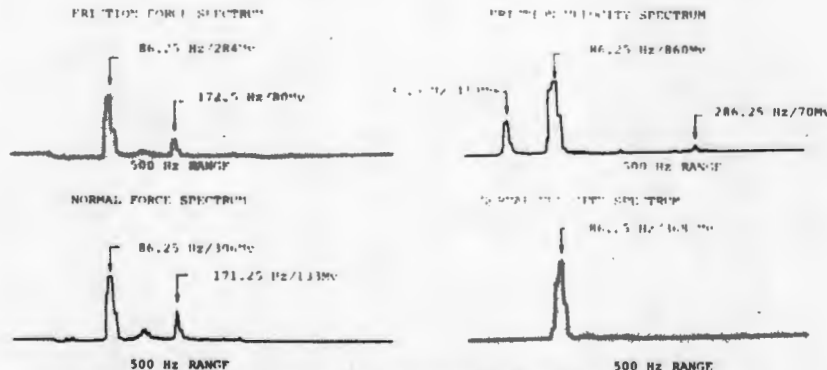


Fig. 6 Spectra of forces and velocities in the region of self-excited vibrations for stiffness K_3 and at a normal load of 110.3 N

oscillations for stiffness K_3 and normal load of 110 N (24.5 lb) are obtained as

$$F_z = 20.16 \sin(2\pi(86.25)t) \text{ N} \quad (1)$$

$$F_x = 78.62 \sin(2\pi(86.25)t) \text{ N} \quad (2)$$

$$V_z = 0.0169 \sin(2\pi(86.25)t - \pi/2 + \gamma_1) \text{ m/s} \quad (3)$$

$$V_x = 0.0360 \sin(2\pi(86.25)t - \pi/2 + \gamma_2) \text{ m/s} \quad (4)$$

where the phase angles γ_1 and γ_2 are too small to be measured accurately from Fig. 5 but are calculated in the next section and shown to be negligibly small. The oscillations in the displacements can be obtained by integrating the velocities as

$$z = 31.55 \times 10^{-6} \sin(2\pi(86.25)t + \pi + \gamma_1) \text{ m} \quad (5)$$

and

$$x = 67.3 \times 10^{-6} \sin(2\pi(86.25)t + \pi + \gamma_2) \text{ m} \quad (6)$$

Since the mean value of the normal load was 110.25 N (24.5 lb), it is seen that the slider does not lose contact with the disk during the self-excited vibrations for stiffness K_3 . Also, since the mean value of the sliding speed is 0.39 m/s, the relative speed between the disk and the pin does not change direction during the vibrations.

Analysis of Self-Excited Vibrations

The dynamic system is modeled as a coupled degrees of freedom system in order to simulate the essential experimental features. A mathematical model of the system is shown in Fig. 1. The slider is represented by three degrees of freedom, namely translation in the x and z directions and torsional rotation about the vertical y axis. The disk is a large mass which is very rigidly supported. Hence no degree of freedom is assigned to the disk except the rotation about its axis at a constant speed.

The slider subsystem is represented by a single body of mass m and moment of inertia I about a central axis y through its mass center. Let K_x , K_z , K_t and C_x , C_z , C_t , be the stiffness and damping coefficients in the x , z , and torsional directions, respectively. For small displacements, the structure behaves quite linearly and retains only the fundamental frequencies of the coupled modes, the equations of motion may be represented as

$$m\ddot{x} + C_x\dot{x} + K_x x = F_x \cos\phi + F_z \sin\phi \quad (7)$$

$$m\ddot{z} + C_z\dot{z} + K_z z = -F_x \sin\phi + F_z \cos\phi \quad (8)$$

$$I\ddot{\phi} + C_t\dot{\phi} + K_t \phi = aF_x \quad (9)$$

where a is the moment arm of F_x as shown in Fig. 1. The forces F_x and F_z can in general be nonlinear functions of the steady state sliding velocity V , the steady state normal force f_z , and of the displacement x , z , ϕ and their time derivatives. For small angle ϕ , $\cos\phi = 1$ and $\sin\phi = 0$. With this approximation, and after employing the natural frequencies and damping ratios, we obtain

$$\ddot{x} + 2\xi_x \omega_{nx} \dot{x} + \omega_{nx}^2 x = (1/m)F_x \quad (10)$$

$$\ddot{z} + 2\xi_z \omega_{nz} \dot{z} + \omega_{nz}^2 z = (1/m)F_z \quad (11)$$

$$\ddot{\phi} + 2\xi_t \omega_{nt} \dot{\phi} + \omega_{nt}^2 \phi = (a/I)F_x \quad (12)$$

The self-excited oscillations are now analyzed for stiffness K_3 . Substituting in (10) for F_x from (2) and for x and its derivatives from (6), letting $\cos\omega t = j \sin\omega t$ in the frequency domain, and equating separately the real and imaginary parts of the resulting equation, we obtain two equations in two unknowns, γ_2 and m . Solution of the equations with the parameter values of Table 1 yields $\gamma_2 = 0.19$ deg and $m = 4.7$ kg. The equivalent mass m was calculated independently to be 4.3 kg. The first two terms on the left hand side of (11) are

negligible since the natural frequency ω_{nz} is very high. This implies that γ_1 is negligible.

Hence phase angles γ_1 and γ_2 are very small and may be neglected. In that case, the phase angle between the force F_z and velocity V_z is π rad. The phase angle between F_x and V_x is also π rad/s. Hence, the net work done per cycle by the oscillating forces in the normal and frictional directions is zero and the instability that gives rise to self-excited vibrations does not occur in those modes. The amplitude and phase angle of the torsional oscillation were not measured but are calculated as follows. Let

$$\phi = \phi_0 \sin(\omega_{nt} t + \gamma_t) \quad (13)$$

where the amplitude ϕ_0 and phase angle γ_t are unknown but the frequency of oscillations ω_{nt} is equal to the torsional natural frequency and is known.

Substituting in (12) for F_x from (2) and for ϕ and its derivatives from (13), and following the preceding procedure employed for the determination of phase angles, we obtain $\phi_0 = 0.128$ rad and $\gamma_t = -\pi/2$. The parameter values $a = 0.03835$ m and $I = 0.0069$ m²kg have been employed in (12). Hence, we obtain

$$\phi = 0.128 \sin\left[2\pi(86.25)t - \frac{\pi}{2}\right] \text{ rad} \quad (14)$$

and thus it follows that

$$\dot{\phi} = 69.366 \sin[2\pi(86.25)t] \quad (15)$$

It is now clear that forces F_z and F_x are in phase with each other and also with $\dot{\phi}$. We may then assume the relationships

$$F_z = c_1 \dot{\phi} \text{ and } F_x = c_2 \dot{\phi} \quad (16)$$

where from (2) and (15), we obtain $c_2 = 1.133$ N.s. Equation (12) now becomes

$$\ddot{\phi} + 2\pi\dot{\phi} + \omega_{nt}^2 \phi = 6.299\dot{\phi}$$

i.e.,

$$\ddot{\phi} - 0.016\dot{\phi} + \omega_{nt}^2 \phi = 0 \quad (17)$$

Inspection of (17) reveals that it is unstable. The linear relationship of (16) requires modification when ϕ is large. A nonlinear relationship is required which limits the growth of ϕ . The self-excited vibrations can then be analyzed by the method of describing functions [10]. This development is currently under study.

The work done per cycle to supply energy to the oscillations can be calculated as

$$W_s = \int_0^{2\pi/\omega} aF_x \dot{\phi} dt \quad (18)$$

After substituting in (18) from (2) and (15) and performing the integration, we obtain $W_s = 1.21$ Joule/cycle. The energy dissipated by cycle is obtained as

$$W_d = \int_0^{2\pi/\omega} 2\xi_t \omega_{nt} I \dot{\phi}^2 dt = 1.20 \text{ Joule/cycle}$$

Very negligible energy is supplied to and dissipated by the normal and frictional modes of vibration. Hence, the energy supplied and dissipated by the fundamental component of the oscillations are in balance.

Conclusions

The paper presents the results of a study of vibrations induced by dry friction. The following conclusions can be drawn from this study.

1) Depending on the normal load, the following four regions of vibrations are encountered in dry friction experiments: vibrations induced by surface irregularities in the

region of steady state friction, vibrations in the regions of nonlinear and transient friction, and self-excited periodic vibrations.

2) The coupling among the different degrees of freedom is an important consideration in self-excited vibrations.

3) The frequency of self-excited vibrations was observed to be the torsional natural frequency of the system. The torsional mode is mainly responsible for the cause of the self-excited vibrations.

4) The energy supplied to maintain the vibrations is mainly through the torsional mode. This energy is then dissipated per cycle by the damping.

5) The experimental results of self-excited vibrations can be partly explained by a simple linear analysis but further study is desirable to understand the relationships and develop a nonlinear theory.

Acknowledgments

This study was sponsored by the U.S. Department of Energy, Contract No. DE-AC02-82ER12071 on "Interactions Between Friction-Induced Vibration and Wear." We would like to thank Dr. Oscar P. Manley of the Division of Engineering, Mathematical and Geosciences, U.S. Department of Energy, for his support of this project. Thanks are also due to Mr. F. Dream, former graduate student, for his assistance. This paper is based partly on the Ph.D. dissertation of I. Shareef.

References

- 1 Ko, P. L., and Brockley, C. A., "The Measurement of Friction and Friction-Induced Vibration," *ASME JOURNAL OF LUBRICATION TECHNOLOGY*, Oct. 1970, pp. 543-549.
- 2 Brockley, C. A., Cameron, R., and Potter, A. F., "Friction Induced Vibration," *ASME JOURNAL OF LUBRICATION TECHNOLOGY*, Apr. 1967, pp. 101-108.
- 3 Soom, A., and Kim, C., "Interaction Between Dynamic Normal and Frictional Forces During Unlubricated Sliding," *ASME JOURNAL OF LUBRICATION TECHNOLOGY* (in press).
- 4 Soom, A., and Kim, C., "Roughness-Induced Dynamic Loading at Dry and Boundary-Lubricated Sliding Contacts," *ASME JOURNAL OF LUBRICATION TECHNOLOGY*, (in press).
- 5 Aronov, V., D'Souza, A. F., Kalpakjian, S., and Shareef, I., "Experimental Investigation of the Effect of System Rigidity on Wear and Friction-Induced Vibrations," *ASME JOURNAL OF LUBRICATION TECHNOLOGY*, Apr. 1983, pp. 206-211.
- 6 Brockley, C. A., and Ko, P. L., "Quasi-Harmonic Friction Induced Vibration," *ASME JOURNAL OF LUBRICATION TECHNOLOGY*, Oct. 1970, pp. 550-556.
- 7 Krauter, A. I., "Generation of Squeal/Chatter in Water Lubricated Elastomeric Bearings," *ASME JOURNAL OF LUBRICATION TECHNOLOGY*, July 1981, pp. 406-413.
- 8 Yokoi, M., and Nakai, M., "A Fundamental Study of Friction Noise," *Bulletin of J.S.M.E.*, Vol. 22, No. 173, 1979, pp. 1665-1671.
- 9 Jarvis, R. P., and Mills, B., "Vibrations Induced by Dry Friction," *Proc. of the Inst. of Mech. Engrs.*, Vol. 178, Part 1, 1963-1964, pp. 847-866.
- 10 Gelb, A., and Vander Velde, W. E., *Multiple-Input Describing Functions and Nonlinear System Design*, McGraw-Hill, New York, 1968.
- 11 Aronov, V., D'Souza, A. F., Kalpakjian, S., and Shareef, I., "Interactions Among Friction, Wear and System Stiffness—Part I: Effect of Normal Load and System Stiffness," *ASME JOURNAL OF LUBRICATION TECHNOLOGY*, (to appear).
- 12 Earles, S. W. E., and Lee, C. K., "Instabilities Arising From the Frictional Interaction of a Pin-Disk System Resulting in Noise Generation," *ASME Journal of Engineering for Industry*, Feb. 1976, pp. 81-86.

APPENDIX 4



The Society shall not be responsible for statements or opinions advanced in papers or in discussion at meetings of the Society or of its Divisions or Sections, or printed in its publications. Discussion is printed only if the paper is published in an ASME Journal. Released for general publication upon presentation. Full credit should be given to ASME, the Technical Division, and the author(s). Papers are available from ASME for nine months after the meeting.
Printed in USA.

V. Aronov
A. F. D'Souza
S. Kalpakjian
I. Shareef

Department of Mechanical Engineering,
Illinois Institute of Technology,
Chicago, Ill. 60616

Interactions Among Friction, Wear, and System Stiffness— Part 3: Wear Model

It is shown that wear is an increasing function of system stiffness. The increase in the frequency of the applied load oscillations in normal direction causes increase of number of loading cycles per unit time that, in turn, causes increased rate of wear particles formation due to fatigue. A wear model has been developed which accounts for slider oscillation in the normal direction. Experimental data correlate very well with the theoretical analysis.

Introduction

The companion papers [1] and [2] of this paper deal with the general description of the sliding contact friction system behavior and the onset of self-excited vibrations. In this paper, attention is concentrated on the region which is commonly called steady state friction, usually associated with lowest rate of wear (mild wear). Dry sliding contact bearings, guides, cams and other frictional elements are expected to perform in this region. Vibration of the friction element members, induced by friction process, may produce adverse conditions of loss of performance and proper functioning.

Recently a few publications have appeared in the literature on the effect of system stiffness on wear in sliding contact. Using a titanium pin sliding against a stainless steel disk, Rice et al. [3] showed that the surface roughness and material loss of the pin increases with increasing pin stiffness. It was further shown that differing phenomenological wear behavior could occur due to variation of stiffness. Kato et al. [4] investigated the effect of system stiffness on wear and vibrations. They concluded that wear of steel against steel is higher for a stiff system as compared to that obtained by the elastic system, while for frictional pairs, such as bronze-steel and white metal-steel, wear tends to decrease with increasing stiffness. Investigating the effect of contact vibrations Miyagawa et al. [5] showed that frictional vibrations increased wear. The subject of normal vibrations and stiffness on contact friction has been investigated by several authors [6-9] and occasionally a reference to vibrational or stiffness phenomena in simulative wear testing is also found in the literature [10]. However, no attempt has been made to investigate the effect of system stiffness on wear and to quantitatively relate wear and vibrations. In a recent investigation by the authors of this paper [11], it was found that, for water lubricated steel-steel pair, mild wear rate increases with an increase in system stiffness.

This paper presents experimental results and theoretical

analysis of the processes involved in formation of wear particles, in the region of mild wear corresponding to the region of steady state friction discussed in companion paper [1]. A wear model is developed based on the concept of fatigue failure due to asperity interactions in the contact region between sliding bodies. A wear equation is derived which relates wear to the frequency of load variation in normal direction. It is found that there is a good agreement between the developed wear equation and the experimental data.

Experimental Procedure

The apparatus, instrumentation and the testing techniques are described in detail in companion paper [1]. The materials of the pin and disk were also the same except that the pin was quenched and hardened to HRC 39. The elastic properties of the pin and disk materials are listed in Table 1.

To investigate the effect of system stiffness different sample arm lengths were used. The stiffnesses and their corresponding arm lengths, and the natural frequencies of vibration in the normal direction with pin not in contact with the disk are given in Table 2. The table also includes the

Table 1

Mating Part	Young's modulus E (GPa)	Poisson's ratio ν
Pin	207	0.3
Disk	103	0.26

Table 2 Natural frequencies

Arm length (cm)	Natural frequency (Hz)	Dominant frequency (Hz)
5	68.75	178.75
6	62.50	183.75
7	56.25	160.00
8	52.50	161.25
9	47.50	148.75
10	43.75	141.25
11	40.00	137.50

Contributed by the Lubrication Division of THE AMERICAN SOCIETY OF MECHANICAL ENGINEERS for presentation at the ASME/ASLE Joint Lubrication Conference, Hartford, Conn., October 18-20, 1983. Manuscript received by the Lubrication Division, March 27, 1983. Paper No. 83-Lub-36. Copies will be available until July 1983.

dominant (highest amplitude) frequency which occurred during the course of the experiments.

In all experiments the pin and disk were lapped in situ by 600 grit-size lapping compound at 20 N normal load and at 60 cm/s sliding speed. Under the same load and speed the pin was run-in for 4 hours over a distance of approximately 8.6 km. During this time the friction force was stabilized and a steady state friction process was achieved.

After the running in period the pin was removed and its surface was analyzed on a Talysurf 10 profilometer by taking three traces of the surface along the friction path. The surface roughness parameter R_a (centerline average) was taken at least four times along each trace. The pin surface was then examined under a light microscope and was weighed accurately (correct to five decimal places of a gram) and replaced back in the same position.

Under the same load and speed conditions the pin was worn for 8 hours which corresponds to a sliding distance of about 17 km at a nominal pressure of 1.02 MPa. After the experiment was completed the pin was removed and the sample was again analyzed in the same way. The difference in weight before and after the experiment was taken as wear.

Experimental Results

The wear per unit traveling distance versus arm length is plotted in Fig. 1. It can be seen that wear increases with decreasing arm length. Wear debris are mostly black with some of brownish color which indicates a mixture of Fe_3O_4 and Fe_2O_3 oxides. The surface roughness, as well as amplitude of normal force vibration, is practically independent of the sample arm length, Figs. 2 and 3.

The center line average of heights (R_a) of asperities range from 0.012×10^{-3} to 0.034×10^{-3} mm. Assuming normal distribution of asperity heights the rms value is calculated to be $rms = R_a/(2)^{1/2} = 0.026 \times 10^{-3}$ mm. The typical wave shape of normal force oscillation is shown in Fig. 4. This wave shape and spectral analysis of the force oscillation show that there is a considerable periodic component of oscillation.

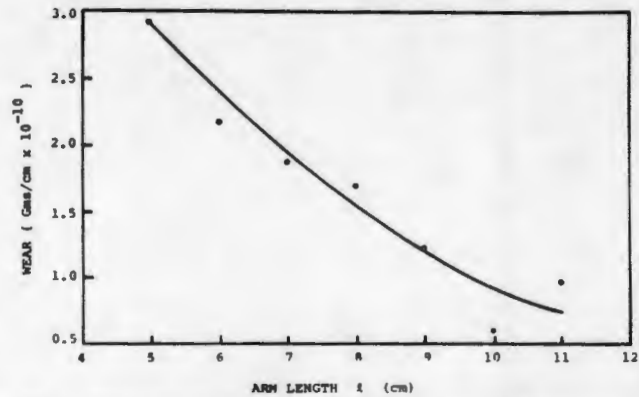


Fig. 1 Wear per unit sliding distance versus supporting arm length

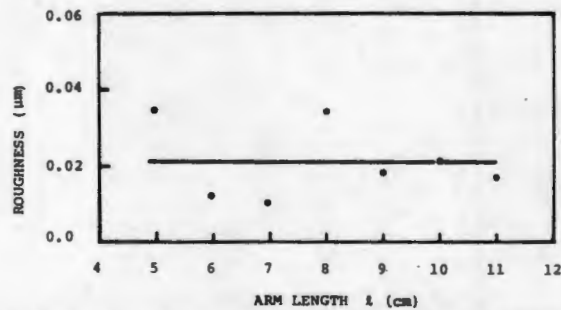


Fig. 2 Surface roughness along the direction of travel versus supporting arm length

The dominant frequency of slider vibration in the normal direction during friction is listed in Table II for each arm length.

Analysis of these data has shown that the increase in wear with stiffness is only associated with a change in the frequency of oscillation of the supporting arm. The shorter the arm the

Nomenclature

- A_0 = apparent contact area
- A_r = real contact area
- A_s = single area transmitting load
- A_t = total area transmitting load
- E_1, E_2 = modulus of elasticity of body 1 and 2
- E' = effective modulus of elasticity
- $$1/E' = \frac{1-\nu_1^2}{E_1} + \frac{1-\nu_2^2}{E_2}$$
- N_f = number of loading cycles required to produce a wear particle
- N_T = number of loading cycles that each area A_s is subjected during time t
- P = applied load
- rms = root mean square
- R_a = centerline average
- R^2 = correlation coefficient
- S = standard error of the estimate of y on x
- T = time during which all population of areas A_s are engaged on the apparent area A_0 to transmit load
- V = sliding velocity
- V_w = volume of a wear particle
- W = wear in time t
- a, b = constants of linear equation
- d = separation between surfaces 1 and 2
- $f = 1/\tau$ = frequency of load variation

- $f_s = 1/\tau_s$ = frequency with which areas A_s are engaged to transmit load
- h = nondimensional parameter $h = d/\sigma$
- l = arm length
- l_1 = distance travelled by area A_s during time τ_s
- $m = \tau/\tau_s$ = number of areas A_s that were engaged to transmit load during time
- n = number of contacts
- n_0 = number of areas A_s that transmit load at time $t = 0$
- n_T = total number of areas A_s on the apparent contact area $n_T = A_0/A_s$
- n_r = cumulative number of areas A_s during time τ
- t = time
- z = size of a wear particle
- β = effective radius of asperity
- $$\beta = \frac{\beta_1 \beta_2}{\beta_1 + \beta_2}$$
- β_1, β_2 = average radius of asperities on the surfaces of body 1 and 2
- η = density of asperities per unit area
- ν_1, ν_2 = Poisson's ratio for body 1 and 2
- ρ = density of wear particles
- σ = standard deviation
- τ = time period of load variation
- τ_s = time during which the area A_s is transmitting load
- ω = wear per travelling length

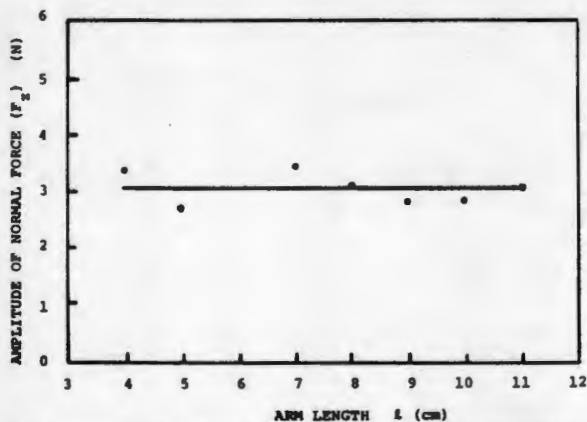


Fig. 3 Amplitude of normal force oscillation versus supporting arm length

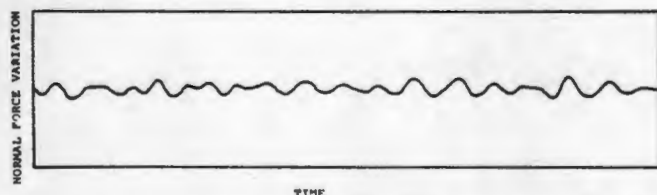


Fig. 4 A typical visicorder trace of the normal force variation at $P = 20$ N and $l = 7$ cm

higher the frequency of oscillation. This effect of frequency on the wear rate can be explained by relating wear to the number of loading cycles. The increase in frequency of normal load oscillation causes an increase in number of loading cycles per unit time. In this case the most probable mechanism of wear particles formation is a fatigue mechanism. The following is a wear model which takes into account the oscillation of the slider in the normal direction.

Wear Model

Considering two rough surfaces in sliding contact, Fig. 5, the contacting surfaces are divided into two distinguishable parts; apparent area (A_0) of contact and area (A_t) which is involved in transmitting load. This latter area is comprised of a number of smaller areas (A_s) to form the total area (A_t) that transmits load at any instance of time.

The following assumptions have been made:

- 1) The number (n_0) of areas (A_s) that transmit the load is directly proportional to the applied load.
- 2) The probability for any elemental area on the surface to be involved in transmitting load is equally distributed over sample area (A_0) and time.
- 3) For any area (A_s) the next consequent involvement in load transmission can be made after all the rest of the area has been engaged.
- 4) The density of the area A_s on the area A_t at any instance of time, equals to the density of the total number of areas A_s on the area A_0 .

If the applied load is constant, the average number of areas (n_0) is constant. The n_0 number of areas A_s are spread over area A_t . For constant sliding velocity V , the average duration of load transmission by the area A_s is τ_s . During this time, the new set of n_0 areas A_s forming area A_t will support load. For varying loads, this number (n_0) of areas A_s will be proportional to load.

For a sinusoidally varying load, the number of areas A_s at any instant of time is

$$n = n_0 + \frac{\Delta n_0}{2} \sin \omega t \quad (1)$$

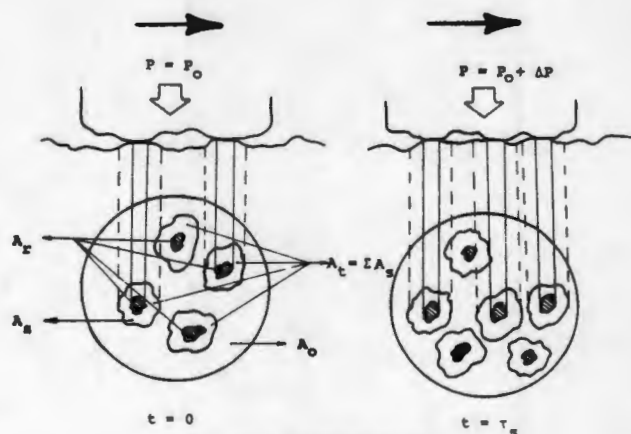


Fig. 5 Surface model

The cumulative number of areas A_s during time period τ of load variation is n_τ . At time $\tau=0$, the number of areas A_s is n_0 . After time τ_s has elapsed the cumulative number of areas A_s becomes

$$n_0 + \left(n_0 + \frac{\Delta n_0}{2} \sin \omega \tau_s \right)$$

For the second period of time τ_s , the cumulative number of areas A_s is

$$n_0 + \left(n_0 + \frac{\Delta n_0}{2} \sin \omega \tau_s \right) + \left(n_0 + \frac{\Delta n_0}{2} \sin \omega 2\tau_s \right)$$

and during time τ

$$\begin{aligned} n_\tau &= n_0 + \left(n_0 + \frac{\Delta n_0}{2} \sin \omega \tau_s \right) \\ &+ \left(n_0 + \frac{\Delta n_0}{2} \sin \omega 2\tau_s \right) + \dots + \left(n_0 + \frac{\Delta n_0}{2} \sin \omega m\tau_s \right) \\ &= (m+1)n_0 + \frac{\cos \frac{\omega \tau_s}{2} - \cos \frac{2m+1}{2} \omega \tau_s}{2 \sin \frac{\omega \tau_s}{2}} \end{aligned} \quad (2)$$

where $m = \frac{\tau}{\tau_s}$

Substituting for m in equation (2), the cumulative number of areas A_s during period τ becomes

$$n_\tau = n_0 \left(1 + \frac{\tau}{\tau_s} \right) = n_0 \tau \left(\frac{1}{\tau} + \frac{1}{\tau_s} \right) \quad (3)$$

where $1/\tau$ is frequency f of load variation and $1/\tau_s$ is frequency f_s with which every single area A_s is involved in supporting the load. For all population of areas A_s to be engaged in load transmission, a period of time T is required. During this time, the load will make T/τ cycles. Taking into account assumption 3 above, the ratio $T/\tau = n_T/n_0$, so that

$$T = \frac{n_T \tau}{n_0} \quad (4)$$

Every area A_s will be subjected to N_T number of loading cycles during any time t , so that

$$N_T = \frac{t}{T} = \frac{t n_0}{n_T \tau} = \frac{n_0}{n_T} t (f + f_s) \quad (5)$$

According to assumption 4,

$$\frac{n_0}{n_T} = \frac{A_t}{A_0}$$

Thus,

$$N_T = \frac{A_i}{A_0} t(f + f_s) \quad (6)$$

If N_f is an average number of loading cycles to produce wear particles of mass ρV_w then

$$W = \frac{N_T}{N_f} \rho V_w = \frac{A_i}{N_f A_0} t(f + f_s) \rho V_w \quad (7)$$

For constant speed, $t = L/V$, so that wear ω per unit distance is

$$\omega = \frac{W}{L} = \frac{A_i}{N_f A_0 V} (f + f_s) \rho V_w \quad (8)$$

Discussion

From an examination of experimental results and equation (8), it is seen that the quantities A_i , f_s , N_f , A_0 , and V are constants. Assuming that average mass of wear particle is independent of the slider oscillation, equation (8) can be represented by the linear equation of the form

$$\omega = a + bf \quad (9)$$

where

$$a = \frac{A_i \rho V_w}{N_f A_0 V} f_s \quad (10)$$

and

$$b = \frac{A_i \rho V_w}{N_f A_0 V} \quad (11)$$

The results of the least square method fit to the experimental data are shown in Table 3 and in Fig. 6.

As can be seen from Table 3 that the constant a is a negative number. This means that this statistical analysis is valid only for $a + bf \geq 0$. In the following analysis only the absolute value of this constant is used.

$$\tau_s = |b/a| = 0.857 \times 10^{-2} \text{ s}$$

For the sliding speed of 60 cm/s, the travelling distance $l_1 = 0.51$ cm. This means that any particular area A_s on the sample surface is transmitting load during a travelling distance of 0.51 cm.

Using this data, it is possible to evaluate the number of cycles required to form a wear particle. Assuming that each area A_s is associated with a single contact and represents a single contact area, the real area of contact A_r is equal to area A_s .

For exponential distribution of the heights of the asperities, the real area of contact is given by

$$A_r = \pi \eta \beta \sigma e^{-h} \quad (12)$$

so that equation (8) is rewritten as

$$\omega = \frac{P(\pi\beta)^{1/2} \rho V_w}{N_f \sigma E' A_0 V} (f + f_s) \quad (13)$$

from which

$$a = \frac{P(\pi\beta)^{1/2} \rho V_w f_s}{N_f \sigma E' A_0 V} \quad (14)$$

and

$$N_f = \frac{P \rho V_w}{\sigma E' A_0 V} \left(\frac{\pi\beta}{\sigma} \right)^{1/2} f_s \quad (15)$$

In this formula only, β , ρ , and V_w are unknown.

For oxide (Fe_2O_3) wear particles, let us assume $\rho = 5.25$ gm/cc. Let us further assume that l_1 is the diameter of an effective area that is subjected to loading during time τ_s . Thus,

Table 3

	a	b	R^2	S
Dominant Frequency	-4.6×10^{-10}	3.94×10^{-12}	0.85	2.7×10^{-11}

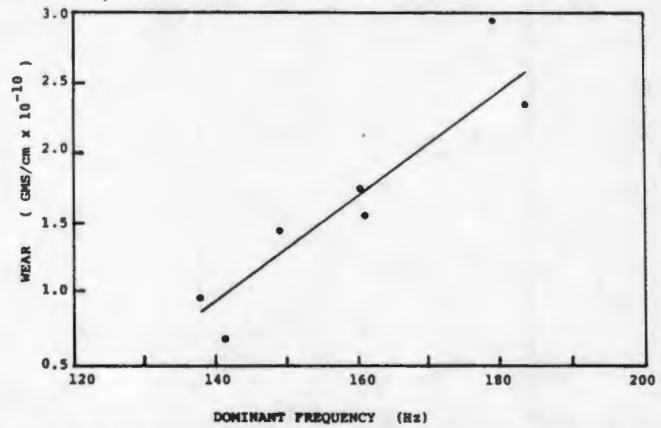


Fig. 6 Wear versus natural frequency of slider oscillation in normal direction

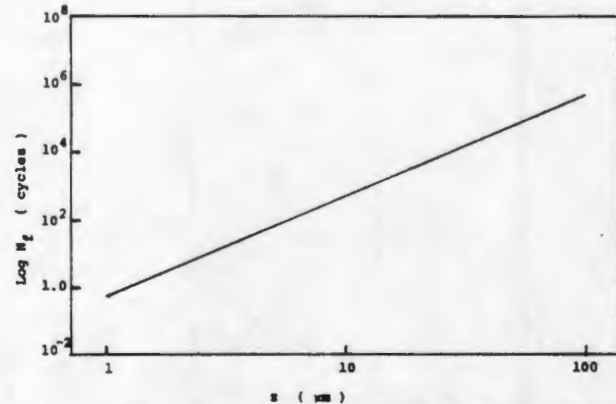


Fig. 7 Number of loading cycles for failure versus size of the wear particles

$$\tau_s = \frac{l_1}{V} = \frac{2/A_r / (\pi n_0)^{1/2}}{V} = \frac{2\sqrt{\beta\sigma}}{V}$$

and

$$\beta = \frac{l_1^2}{4\sigma} = 2.47 \times 10^4 \text{ cm}$$

This radius is an effective radius of two combined surface asperities and is given as

$$\frac{1}{\beta} = \frac{1}{\beta_1} + \frac{1}{\beta_2}$$

Assuming that $\beta_1 = \beta_2$, the effective radius β is given by

$$\beta = \frac{1}{2} \beta_1 = 1.24 \times 10^4 \text{ cm}$$

For the materials used in the investigation, the effective Young's modulus E' is equal to 74.6 GPa. The volume of a wear particle is proportional to the third power of its size z . With this data, the number of cycles N_f required to form a wear particle is evaluated for wear particle size varying from 1×10^{-3} mm to 100×10^{-3} mm. This is shown in Fig. 7.

As can be seen from this figure, approximately every loading cycle may generate a wear particle of $1 \mu\text{m}$ average size or it requires around 10^5 cycles to form a wear particle of $100 \mu\text{m}$.

In our investigation a systematic analysis of the wear particle size distribution was not carried out. However, the wear particles randomly collected from different wear experiments were analyzed on an optical microscope. From this analysis the size distribution of wear particles was found to be between 10 μm to 100 μm . This means that, most probably the wear particles in these friction and wear experiments were formed by a low cycle fatigue mechanism.

Conclusions

A wear model is developed which accounts for slider oscillations in the normal direction. The experimental investigation of the wear dependence on system stiffness has shown that the increase in wear rate is associated with increase of frequency of the slider oscillation in the normal direction when system stiffness is increased. The proposed model sufficiently fits the experimental data.

Acknowledgments

This study was sponsored by the U.S. Department of Energy, Contract No. DE-AC02-82ER12071 on "Interactions Between Friction-Induced Vibration and Wear." We would like to thank Dr. Oscar P. Manley of the Division of Engineering, Mathematical and Geosciences, U.S. Department of Energy, for his support of this project. This paper is based partly on the Ph.D. dissertation of I. Shareef.

References

- 1 Aronov, V., D'Souza, A. F., Kalpakjian, S., and Shareef, I., "Interactions Among Friction, Wear and System Stiffness - Part 1: Effect of Normal Load and System Stiffness," *ASME JOURNAL OF LUBRICATION TECHNOLOGY* (to appear).
- 2 Aronov, V., D'Souza, A. F., Kalpakjian, S., and Shareef, I., "Interactions Among Friction, Wear and System Stiffness - Part 2: Vibrations Induced by Dry Friction," *ASME JOURNAL OF LUBRICATION TECHNOLOGY* (to appear).
- 3 Rice, S. L., Hans, N., and Steven, F. W., "The Role of Specimen Stiffness in Sliding and Impact Wear," *WEAR*, Vol. 77, 1982, pp. 13-28.
- 4 Kato, K., Iwabuchi, A., and Kayaba, T., "The Effects of Friction-Induced Vibration on Friction and Wear," *WEAR*, Vol. 80, 1982, pp. 307-320.
- 5 Miyagawa, Y., Seki, K., and Nishimura, T., *Jpn. Soc. Lubr. Engg.*, Vol. 18, 1973, pp. 323, (in Japanese).
- 6 Tolstoi, M., "Significance of the Normal Degree of Freedom and Natural Normal Vibrations in Contact Friction," *WEAR*, Vol. 10, 1967, pp. 199-213.
- 7 Broszeit, E., Kloos, K. H., Hess, F. J., and Wagner, E., "Influence of Vibrations on the Wear Properties on a Tribological System," *WEAR*, Vol. 28, 1974, pp. 395-401.
- 8 Elder, J. A., and Eiss, N. S., "A Study of the Effect of Normal Stiffness on Kinetic Friction Forces Between Two Bodies in Sliding Contact," *ASME JOURNAL OF LUBRICATION TECHNOLOGY*, 1969, pp. 234-241.
- 9 Budanov, B. V., Kudinov, V. A., and Tolstoi, D. M., "Interaction of Friction and Vibration," *Trenie i Iznos*, Vol. 1, 1980, pp. 79-89. (Russian).
- 10 Soda, N., Kimura, Y., and Tanaka, A., "Wear of Some f.c.c. Metals During Unlubricated Sliding. Part I: Effects of Load, Velocity and Atmosphere Pressure on Wear," *WEAR*, Vol. 33, 1975, pp. 1-16.
- 11 Aronov, V., D'Souza, A. F., Kalpakjian, S., and Shareef, I., "Experimental Investigation of the Effects of System Rigidity on Wear and Friction-Induced Vibrations," *ASME JOURNAL OF LUBRICATION TECHNOLOGY*, April 1983, pp. 206-211.